

Graph Neural Networks Are Evolutionary Algorithms

Kaichen Ouyang^{1,*}, Shengwei Fu²

¹Department of Mathematics, University of Science and Technology of China, Hefei 230026, China

²Key Laboratory of Advanced Manufacturing Technology, Ministry of Education, Guizhou University, Guiyang, Guizhou, China 550025

*Corresponding author(s). E-mail(s): oykc@mail.ustc.edu.cn

Abstract

In this paper, we reveal the intrinsic duality between graph neural networks (GNNs) and evolutionary algorithms (EAs), bridging two traditionally distinct fields. Building on this insight, we propose Graph Neural Evolution (GNE), a novel evolutionary algorithm that models individuals as nodes in a graph and leverages designed frequency-domain filters to balance global exploration and local exploitation. Through the use of these filters, GNE aggregates high-frequency (diversity-enhancing) and low-frequency (stability-promoting) information, transforming EAs into interpretable and tunable mechanisms in the frequency domain. Extensive experiments on benchmark functions demonstrate that GNE consistently outperforms state-of-the-art algorithms such as GA, DE, CMA-ES, SDAES, and RL-SHADE, excelling in complex landscapes, optimal solution shifts, and noisy environments. Its robustness, adaptability, and superior convergence highlight its practical and theoretical value. Beyond optimization, GNE establishes a conceptual and mathematical foundation linking EAs and GNNs, offering new perspectives for both fields. Its framework encourages the development of task-adaptive filters and hybrid approaches for EAs, while its insights can inspire advances in GNNs, such as improved global information propagation and mitigation of oversmoothing. GNE's versatility extends to solving challenges in machine learning, including hyperparameter tuning and neural architecture search, as well as real-world applications in engineering and operations research. By uniting the dynamics of EAs with the structural insights of GNNs, this work provides a foundation for interdisciplinary innovation, paving the way for scalable and interpretable solutions to complex optimization problems.

1. Introduction

The core characteristic of complex systems lies in their multi-agent interactions and adaptability, enabling the emergence of global patterns from local behaviors. Neural networks can be viewed as a type of complex system, composed of interacting neurons[1-3]. These neurons influence each other through intricate weights, biases, and nonlinear activation functions, thereby facilitating the transmission and processing of information[4-7]. Similarly, the process of biological evolution can be understood as the interaction and exchange of information between different genes. Through genetic variation, recombination, and natural selection, the evolutionary process gradually optimizes genotypes, ultimately producing individuals with higher fitness[8-10]. This paper posits that graph neural networks (GNNs)[11, 12]—a model based on graph structures that learns node representations by aggregating information from neighboring nodes—can fundamentally be seen as a form of evolutionary process. The information propagation in GNNs mirrors the mechanisms

of diversity generation and adaptive optimization found in the evolution of genotypes.

The evolutionary process, driven by the genetic makeup of species, is a highly complex and adaptive system. Through genetic crossover and mutation, diversity is introduced into the population, enabling the exploration of a broader adaptive space[9, 13, 14]. Simultaneously, existing genes, under the influence of natural selection, evolve toward higher fitness. This dynamic balance—fostering the generation of diversity while guiding the optimization of adaptability—is the core mechanism that sustains evolution[15-17]. Evolutionary algorithms (EAs) abstract and simulate this process by introducing the concepts of "exploration" and "exploitation" to describe this balance[18-22]. Exploration corresponds to genetic crossover and mutation, which generate diverse solutions and broaden the search space, while exploitation mirrors the role of natural selection, refining candidate solutions by guiding them toward regions of higher fitness. Exploration ensures the algorithm avoids being trapped in local optima, while exploitation guarantees that potential regions of the solution space are thoroughly explored. This balance between global search (exploration) and local optimization (exploitation) not only underpins the success of evolutionary algorithms but also represents a universal mechanism in complex adaptive systems. The elegance and effectiveness of this mechanism are evident in biological evolution and have inspired its widespread application in the design of optimization algorithms.

Inspired by the rapid advancements in deep learning in recent years, the balance between global and local processes is similarly reflected in Graph Neural Networks (GNNs)[11, 12, 23, 24]. In GNNs, each node aggregates information from its neighboring nodes to facilitate local information propagation and representation updates. This "local aggregation" process captures the relationships between nodes and the structural characteristics of the data, resembling the adaptation of genotypes to specific environments in evolutionary processes. However, relying solely on local aggregation limits the range of information propagation and can lead to the phenomenon of oversmoothing, where the features of different nodes become increasingly homogenized[25-30]. This phenomenon, to some extent, mirrors the loss of population diversity in evolutionary algorithms—when solutions within a population become overly concentrated around local optima, the algorithm loses its ability to explore broader solution spaces, thereby constraining its potential for global search[31-34]. To address this, GNNs must expand the range of information propagation through a larger receptive field, ensuring the capture of global patterns and achieving a dynamic balance between global exploration and local aggregation[28, 35-42]. This balancing mechanism closely parallels the "exploration and exploitation" trade-off in evolutionary algorithms and raises a profound question: is there a deeper connection between Graph Neural Networks and evolutionary algorithms? Are the similarities they exhibit in solving optimization problems driven by an underlying mathematical duality, or are they merely a phenomenological analogy? In other words, is the information propagation in GNNs and the genetic propagation in evolutionary algorithms merely structurally similar, or do they share a unified theoretical framework at their core?

To address this question, we begin by reinterpreting evolutionary algorithms (EAs) from the perspective of graph neural networks (GNNs). In evolutionary algorithms, individuals can be represented as nodes in a graph, with the interactions between these nodes modeled through an

adjacency matrix. Similar genotypes are more likely to interact, which corresponds to the phenomenon of reproductive isolation in biological evolution. This can be intuitively represented by higher edge weights in the adjacency matrix, where individuals with similar genotypes are more likely to mate and exchange genetic information, while those with significantly different genotypes are less likely to form direct interactions. The node update process in EAs can further be understood as the superposition of information at different frequencies, which corresponds to the information aggregation process in spectral GNNs[11, 12, 43-46]. In EAs, the update of an individual arises from the interaction and exchange of diverse genetic information within the population. This process can be decomposed into two types of frequency contributions: on the one hand, low-frequency information represents the global consistency or stability of the population, reflecting the inheritance of advantageous genes validated during evolution. On the other hand, high-frequency information captures local diversity among individuals, which is introduced through mutation or crossover mechanisms, reflecting genetic variability. The inclusion of high-frequency information provides the necessary exploratory capability for EAs, helping the population avoid becoming trapped in local optima. By designing appropriate interaction and update rules, EAs achieve a dynamic balance between high-frequency and low-frequency information. This balance is critical to the effectiveness of EAs: excessive reliance on low-frequency information leads to homogeneity within the population, resulting in a loss of genetic diversity and limiting the algorithm's ability to explore the solution space. Conversely, overemphasizing high-frequency information amplifies differences between individuals, disrupting global adaptability and preventing the algorithm from focusing on high-fitness regions. Only by appropriately adjusting the contributions of these two types of frequency information can EAs organically combine global exploration and local exploitation within the solution space.

From another perspective, graph neural networks (GNNs) can be viewed as a type of evolutionary algorithm. The process of aggregating high- and low-frequency information bears a striking resemblance to the process of evolution. The aggregation of low-frequency information can be likened to the inheritance of "advantageous traits" in genes during evolution, where existing adaptive traits are retained and reinforced. In contrast, the aggregation of high-frequency information resembles genetic crossover and mutation, introducing new traits with significant variations to enhance the diversity of the population. Spectral-based GNNs achieve this balance between high- and low-frequency information through the design of appropriate filters, which essentially mirrors the "exploration versus exploitation" trade-off in evolutionary algorithms[44, 47-51]. The aggregation of low-frequency information emphasizes exploiting existing advantages, while high-frequency information aggregation expands the scope of exploration in the solution space. Taking this analogy further, each iteration of a GNN can be seen as an adaptive adjustment of the filter's weight distribution between high- and low-frequency information. This weight optimization is dynamically achieved through gradient descent, enabling the GNN to continuously adjust the proportion of high- and low-frequency information based on the specific task requirements. This process reflects the mathematical essence of "directional selection" in evolution, where natural selection determines how much low-frequency stability and high-frequency innovation should be retained or introduced in the population. Taking this analogy further, each iteration of a GNN can be seen as an adaptive adjustment of the filter's weight distribution between high- and low-frequency information. This weight optimization is

dynamically achieved through gradient descent, enabling the GNN to continuously adjust the proportion of high- and low-frequency information based on the specific task requirements. This process reflects the mathematical essence of "directional selection" in evolution, where natural selection determines how much low-frequency stability and high-frequency innovation should be retained or introduced in the population.

Inspired by the above discussion, we delved deeper into the potential connections between graph neural networks (GNNs) and evolutionary algorithms, uncovering profound mathematical correspondences between the two. Based on this discovery, we propose a novel evolutionary algorithm, termed Graph Neural Evolution (GNE). Specifically, we leverage the similarities between individuals to construct an adjacency matrix, modeling the process of individual updates in evolution as a filtering operation on a graph. By designing appropriate filter functions, we can effectively aggregate both global and local information, thereby enhancing the population's search capabilities. More importantly, the ratio of global to local information aggregation during population updates can be explicitly represented using polynomial functions. This not only enhances the interpretability of evolutionary algorithms, traditionally considered black-box models, but also provides theoretical support for further optimization and analysis.

This duality bridges the seemingly independent fields of graph neural networks (GNNs) and evolutionary computation, enabling mutual inspiration and cross-disciplinary learning. The proposed GNE algorithm introduces an innovative framework for designing evolutionary algorithms, redefining the core process of "exploration and exploitation" from a frequency-domain perspective. By treating the superposition of different frequency components in a population as a filtering operation, the design of evolutionary algorithms shifts from traditional spatial-domain update mechanisms to optimizing frequency components in the frequency domain. This transformation not only decouples the update process of evolutionary algorithms from complex nonlinear black-box models but also significantly enhances their interpretability and controllability through the explicit description of the filtering function. Conversely, the node update mechanisms in graph neural networks can also draw inspiration from evolutionary algorithms. For example, incorporating more diverse crossover and mutation operators can enhance the flexibility of information exchange between nodes, mitigating the over smoothing problem and improving the distinctiveness of node representations. This cross-disciplinary interaction not only opens new avenues for the advancement of both fields but also paves the way for modeling more complex systems on a broader scale.

In the following sections, we first systematically review the fundamental principles of evolutionary algorithms and graph neural networks (GNNs), laying a solid foundation for the subsequent theoretical analysis. Next, we delve into the mathematical connections between evolutionary algorithms and GNNs, based on which we propose the GNE (Graph Neural Evolution) algorithm. This innovative framework reconstructs the core processes of evolutionary algorithms from a frequency-domain perspective. We then conduct a detailed analysis of GNE's performance in optimization tasks by comparing it with several classical and widely recognized evolutionary strategies, particularly focusing on its adaptability to scenarios where the optimal solution of the objective function shifts or noise is introduced. Experimental results demonstrate

that GNE not only maintains high convergence efficiency but also dynamically adjusts population information, exhibiting remarkable robustness and flexibility. Additionally, as part of our exploratory research, we analyze the impact of different polynomial-based filter functions on GNE's performance, uncovering the profound influence of filter design on the algorithm's outcomes. This provides valuable insights and directions for further improvements to the GNE model. In the final section, we objectively examine the limitations of GNE and discuss potential areas for improvement. We also explore the future possibilities of integrating evolutionary computation and GNNs, highlighting their potential for mutual development and synergy. This perspective offers new avenues for fostering collaborative innovation between the two fields.

2. Related Works

2.1 Evolutionary Algorithms

Evolutionary Algorithms (EAs) are a class of optimization methods inspired by the biological mechanisms of natural evolution, rooted in Darwin's principle of "survival of the fittest." By simulating processes such as natural selection, genetic recombination, and mutation, EAs operate on a population of solutions to search for the optimal solution in the solution space. The Genetic Algorithm (GA) is one of the earliest and most extensively studied EAs[8]. It utilizes operations such as selection, crossover, and mutation to generate new candidate solutions, performing well in solving discrete and multi-modal optimization problems. However, GA often struggles with slow convergence and susceptibility to local optima when tackling high-dimensional continuous optimization problems. To address these limitations, Differential Evolution (DE) was introduced, leveraging the differences between individuals in the population to generate new solutions, thereby significantly enhancing global search capabilities and optimization efficiency[52]. Subsequently, the Covariance Matrix Adaptation Evolution Strategy (CMA-ES) was developed, dynamically adjusting the covariance matrix to capture the directional distribution of the population, making it particularly effective for high-dimensional continuous optimization problems[53]. More recently, researchers have proposed strategies such as the Search Direction Adaptation Evolution Strategy (SDAES)[54] and Learning Adaptive Differential Evolution by Natural Evolution Strategies (RL-LSHADE)[55], which demonstrate remarkable advantages in dynamically adjusting parameters and search directions for large-scale optimization problems.

From GA to DE, CMA-ES, and more advanced variants, the design of evolutionary algorithms has always centered on the balance between exploration and exploitation, which is the key to their success. Exploration aims to introduce diversity and expand the search space, helping to avoid local optima. Specifically, exploration corresponds to operations like crossover and mutation, which enable broad sampling of the solution space. In contrast, exploitation focuses on refining the search around promising solutions to improve precision and gradually approach the optimal solution. Maintaining this balance between exploration and exploitation is crucial in evolutionary algorithms, as any imbalance may lead to a decline in efficiency.

This dynamic balance between exploration and exploitation can be interpreted through the lens of signal processing, where the update process of evolutionary algorithms is essentially a combination of low-frequency and high-frequency information. Exploration, driven by mutation, resembles the introduction of high-frequency information, which enhances population diversity

and broadens the search space. Exploitation, on the other hand, is akin to low-frequency processing, concentrating on promising regions and reinforcing stable patterns in the population to improve overall fitness. In this sense, the update mechanism of evolutionary algorithms can be seen as a “filtering” process: The high-frequency components preserve the diversity of the population, preventing it from getting trapped in local optima, while the low-frequency components reduce noise and amplify the influence of high-quality genetic information within the population. This process of signal optimization ultimately leads to a steady improvement in the overall fitness of the population, accelerating convergence toward the optimal solution.

2.2 Graph Neural Networks

Graph Neural Networks (GNNs) are a class of deep learning methods designed for processing graph-structured data, aiming to effectively extract and represent features in the non-Euclidean domain of graphs. GNNs are built upon the unique properties of graphs, where nodes and edges represent entities and their relationships, respectively. The study and development of GNNs are primarily conducted from two perspectives: spatial domain and spectral domain[47, 56]. From the spatial perspective, GNNs focus on local aggregation by directly leveraging the neighborhood information of nodes. Through an iterative message-passing mechanism, the representation of each node is updated by aggregating information from its neighbors, gradually learning a more expressive embedding for each node. For instance, the Graph Convolutional Network (GCN)[11], a representative method in the spatial domain, can be mathematically expressed as:

$$H^{(l+1)} = \sigma(\bar{A}H^lW^l)\#(1)$$

where, $\bar{A} = D^{-\frac{1}{2}}\tilde{A}D^{-\frac{1}{2}}$ represents the normalized adjacency matrix, $\tilde{A} = A + I$ denotes the adjacency matrix with added self-loops, D is the degree matrix, $H^{(l)}$ reports the node feature matrix at layer l , $W^{(l)}$ represents the trainable weight matrix, and σ is the activation function.

GCN performs neighborhood aggregation by averaging the features of neighboring nodes, effectively propagating structural information to the central node. However, this simple aggregation mechanism overlooks the varying importance of different neighbors. To address this limitation, the Graph Attention Network (GAT) introduces an attention mechanism to dynamically assign different weights to neighbors[12]. The update rule for GAT is as follows Eq. (2).

$$h_i^{(l+1)} = \sigma\left(\sum_{j \in N(i)} \alpha_{ij} Wh_j^{(l)}\right)\#(2)$$

where α_{ij} denotes the attention weight computed for neighbor j relative to central node i , indicating the importance of node j to node i .

Spatial-based methods are intuitive and flexible, making them widely applicable to many graph tasks such as node classification, link prediction, and graph clustering. However, they primarily rely on local neighborhood information and may struggle to effectively capture global structural properties of the graph.

The spectral perspective approaches GNNs from the frequency domain, utilizing the spectral properties of the graph Laplacian to define convolutional operations on graphs. The graph Laplacian is defined as Eq. (3).

$$L = D - A \#(3)$$

where, D represents the degree matrix and A denotes the adjacency matrix. The normalized Laplacian is further expressed as Eq. (4).

$$L_{norm} = I - D^{-\frac{1}{2}}AD^{-\frac{1}{2}} \#(4)$$

Spectral methods perform graph convolution by applying a graph Fourier transform to signals $x = \{x_1, x_2, \dots, x_N\}$, mapping them to the frequency domain. Specifically, the graph Fourier transform is based on the eigen-decomposition of the Laplacian matrix as Eq. (5).

$$U^T x, \text{ where } L = U\Lambda U^T \#(5)$$

where, U represents the eigenvector matrix of the Laplacian and Λ denotes the diagonal matrix of eigenvalues. The convolution operation in the spectral domain is defined as Eq. (6).

$$y = Ug(\Lambda)U^T x \#(6)$$

where, $g(\Lambda)$ is a filter function applied to the eigenvalues. While spectral methods are theoretically elegant and capture the global structure of the graph, early approaches faced challenges such as high computational cost and poor generalization to graphs with different structures. To overcome these limitations, Chebyshev networks introduced an approximation using Chebyshev polynomials, significantly reducing the computational complexity. The convolution operation is approximated as Eq. (7).

$$g(\Lambda) \approx \sum_{k=0}^K \theta_k T_k(\tilde{L}) \#(7)$$

where, $T_k(\tilde{L})$ represents the Chebyshev polynomial of order k , \tilde{L} is the rescaled Laplacian, and θ_k is Learnable parameters. Based on this, GCN further proposed a first-order approximation, simplifying the computation while maintaining high efficiency. In general, existing spectral-domain-based Graph Neural Networks (GNNs) can be uniformly expressed in Eq. (8)[48].

$$Z = \phi \left(g(\tilde{L}) \varphi(X) \right) \#(8)$$

where, Z represents the prediction, ϕ and φ are functions, such as multi-layer perceptrons (MLPs), and g is a polynomial. Although spatial and spectral methods differ in their starting points

and implementation, they can both be viewed as processes of propagating information between nodes to iteratively update and optimize node representations. During training, the representations are guided by loss functions and optimized through gradient descent, analogous to the evolutionary process of optimizing individuals in a population. If nodes are considered as individuals in a population, the training of GNNs can be seen as an evolution process, where nodes progressively evolve by exchanging information with their neighbors. Compared to spatial methods, spectral methods offer stronger mathematical interpretability due to their reliance on graph frequency characteristics. By leveraging filtering operations in the frequency domain, spectral methods can better capture the global structure of the graph and reveal potential relationships between nodes. As a result, modern GNNs aim to combine the computational efficiency of spatial methods with the interpretability of spectral methods, enabling unified frameworks that effectively model both local and global information.

3. Graph Neural Networks are Evolutionary Algorithms

Similar to how graph neural networks update nodes based on graph structures, evolutionary algorithms can also establish a connection with graph neural networks by constructing a similarity matrix among individuals in the population. In evolutionary algorithms, each individual in the population can be viewed as a node in the graph, while the similarity matrix describes the interactions between these nodes. Individuals with higher similarity can be considered to have more similar genotypes, making them more likely to interact with each other. This mechanism aligns closely with the concept of "reproductive isolation" in biological evolution, where only sufficiently similar individuals are more likely to exchange and transmit genetic information. To ensure that the similarity matrix reflects as much information about the population as possible, the center of the population X_0 is used as a reference point. The similarity between individuals is then measured by calculating the cosine similarity of the difference vectors $Z_i = X_i - X_0$ between each individual X_i and the population center X_0 . The similarity A_{ij} between individual i and individual j is represented as shown in Eq. (9). To ensure numerical stability and computational adaptability, the similarity is further enhanced using an exponential function and normalized accordingly.

$$A_{ij} = \frac{Z_i Z_j}{\|Z_i\| \|Z_j\|} \#(9)$$

After obtaining the similarity matrix A , we can further construct the normalized Laplacian matrix $L_{norm} = I - D^{-\frac{1}{2}} A D^{-\frac{1}{2}}$. Subsequently, we perform spectral decomposition on the Laplacian matrix to obtain the diagonal matrix of eigenvalues $\Lambda = \text{diag}[\lambda_1, \dots, \lambda_N]$ and the corresponding eigenvector matrix $U = [U_1, \dots, U_N]$. Here, λ_t represents the t -th largest eigenvalue, and U_t represents its corresponding eigenvector. The expression for λ_t and U_t , when expanded, can be further detailed as shown in Eq. (10).

$$\lambda_t = \frac{1}{2} \sum_{ij} A_{ij} \left(\frac{U_{ti}}{\sqrt{d_i}} - \frac{U_{tj}}{\sqrt{d_j}} \right)^2 \#(10)$$

where, U_{ti} and U_{tj} represent the components of individuals i and j in the eigenvector U_t , while d_i and d_j denote the degrees of individuals i and j , respectively. A larger λ_t indicates greater variability in the population X along the direction of U_t , which can be interpreted as the frequency of population information in that direction. The transition from low frequencies to high frequencies gradually reflects a shift from global consistency to individual diversity within the population.

In spectral-based graph neural networks, filter $g(\Lambda) \approx \sum_{k=0}^K \theta_k T_k(\tilde{L})$ is typically approximated using polynomials $T_k(\tilde{L})$, where the θ_k are learnable parameters. These parameters represent the rules learned by the graph neural network to assign different weights to different frequency components. In the context of evolutionary algorithms, low-frequency information within a population can be viewed as stable and high-quality genetic information that has been validated through natural selection. On the other hand, high-frequency information represents more distinct genetic components, which can be attributed to genetic recombination and mutation. The process of natural selection can essentially be seen as a filtering mechanism for the population's genetic information, gradually refining the genotype distribution towards one with higher fitness. Similarly, we can define a filter to simulate the role of natural selection in filtering genetic information, as shown in Eq. (11). In Eq. (11), the θ_k is replaced with c_k to reflect the inherent completeness of the natural selection process, emphasizing its ability to efficiently filter population information during evolution without requiring external intervention.

$$g(\Lambda) \approx \sum_{k=0}^K c_k T_k(\tilde{L}) \# (11)$$

By adjusting the c_k of the filter, we can flexibly control the algorithm's focus on different frequency components during the update process. A higher weight on the low-frequency components means that the overall information of the population is more aggregated, enhancing the algorithm's exploitation ability. Conversely, a higher weight on the high-frequency components indicates that more diverse information within the population is being aggregated, thereby improving the algorithm's exploration capability. As a result, the design of the filter function g essentially determines the algorithm's balance and preference between exploration and exploitation. This mechanism not only provides the algorithm with greater flexibility but also enhances its interpretability. To ensure numerical stability, the values of g have been normalized within a specific range. Through Eq. (9)–(11), we effectively complete the filtering process for the evolutionary algorithm's population, with the updated population expressed by Eq. (12).

$$X_{new} = Ug(\Lambda)U^T X \# (12)$$

In Eq. (8), existing spectral-based graph neural networks typically apply nonlinear transformations φ and ϕ to the original feature matrix X or the filtered feature matrix. These transformations are usually functions similar to multi-layer perceptrons (MLPs). During the training process of graph neural networks, the parameters of these nonlinear transformations are continuously updated using the gradient descent algorithm with a specific learning rate. In this process, the changes in φ and

ϕ can be viewed as a resampling operation in their respective feature spaces, where the features are updated along the optimization direction with a certain step size. This resampling process adjusts their distribution gradually to better fit the requirements of specific problems, thereby enhancing the model's representational capability and optimization performance for the target task. Similarly, in evolutionary algorithms, nonlinear transformations φ and ϕ can be implemented by resampling the current population along the optimization direction. This process corresponds to progressively adjusting the population's distribution through resampling, making it more concentrated in high-fitness regions and thus improving the optimization results. The overall update process of the population can be described by Eq. (13), which integrates the ideas of graph neural networks to create a novel evolutionary algorithm—Graph Neural Evolution (GNE). The pseudocode for this algorithm is presented in **Algorithm 1**.

$$X_{new} = \phi(Ug(\Lambda)U^T\varphi(X))\#(13)$$

Algorithm 1 Graph Neural Evolution

Input: Population size N , Maximum iterations T , Objective Function f , Lower Bound LB , Upper Bound UB , Nonlinear Transformation φ, ϕ , Filter g

Initialization: Population X , optimal solution x_{best} , optimal function value f_{best} , $t = 0$

While $t \leq T$

 Apply $\varphi(X)$ to X for nonlinear transformation.

 Calculate the similarity matrix A for the population X

 Calculate the normalized Laplacian matrix L using $L = I - D^{-\frac{1}{2}}AD^{-\frac{1}{2}}$

 Calculate the Diagonal eigenvalue matrix Λ and the eigenvector matrix U of the L

 Obtain the updated population X_{new} through $X_{new} = Ug(\Lambda)U^T X$

 Apply $\phi(X_{new})$ to X_{new} for nonlinear transformation.

$t = t + 1$

 Update the optimal solution x_{best} and the optimal function value f_{best}

End

4. Experimental results and analysis

In this section, we compare the performance of GNE with five well-established and widely recognized evolutionary algorithms: Genetic Algorithm (GA), Differential Evolution (DE), Evolution Strategy with Covariance Matrix Adaptation (CMA-ES), Strategy Based on Search Direction Adaptation (SDAES), and Learning Adaptive Differential Evolution by Natural Evolution Strategies (RL-SHADE). The comparison is conducted on nine classical benchmark functions to evaluate the convergence and robustness of GNE. The detailed descriptions of these benchmark functions, including their mathematical expressions, bounds, dimensions, and characteristics, are provided in **Appendix A.1**. Furthermore, we assess GNE's performance under challenging scenarios, including when the optimal solution of a function is shifted and when noise is added to the function, to verify its generalization capability and resilience to noise. Finally, as an extension, we explore GNE models under different polynomial bases and compare their performance to gain deeper insights into their effectiveness. In Sections 4.1 and 4.2, GNE employs

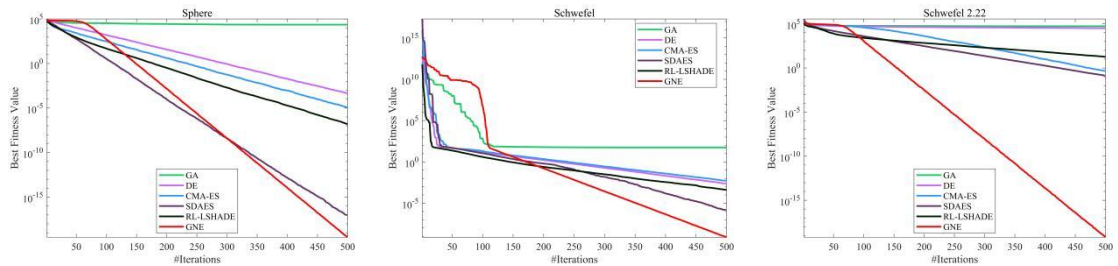
Chebyshev polynomials to approximate the filter function, which plays a pivotal role in balancing high- and low-frequency components during the optimization process. The specific formulation and details of the Chebyshev polynomial-based filters are presented in **Appendix A.2**.

4.1 Comparison of GNE and Other Evolutionary Algorithms

In this section, we compare GNE with five well-established and widely recognized evolutionary algorithms: GA, DE, CMA-ES, SDAES, and RL-SHADE. The comparison is conducted on nine classical benchmark functions: Sphere, Schwefel, Schwefel 2.22, Schwefel 2.26, Rosenbrock, Quartic, Rastrigin, Ackley, and Levy. For each algorithm, the population size N is set to 30, and the maximum number of iterations T is set to 500. Each algorithm is independently executed 30 times, and we calculate the mean and standard deviation of the results.

Table 1 Performance Comparison of GNE with Other Evolutionary Algorithms on Benchmark Functions

Benchmark Functions	index	GA	DE	CMA-ES	SDAES	RL-SHADE	GNE
Sphere	Ave	2.30545E+04	4.52677E-04	1.21994E-05	9.22187E-18	1.51069E-07	3.07339E-20
	Std	7.10445E+03	1.74574E-04	9.27454E-06	1.42731E-17	2.17477E-07	5.26372E-21
Schwefel	Ave	5.59815E+01	2.31056E-03	5.28201E-03	1.53564E-06	4.14287E-04	7.64601E-10
	Std	8.58008E+00	5.82953E-04	1.46233E-03	5.93762E-06	4.99282E-04	4.08476E-11
Schwefel 2.22	Ave	5.42261E+04	3.23819E+04	4.28281E-01	1.34979E-01	1.84913E+01	6.39796E-20
	Std	1.37592E+04	5.30798E+03	2.33492E-01	9.86213E-02	1.50665E+01	1.33486E-20
Schwefel 2.26	Ave	7.21591E+01	1.25354E+01	2.34950E-02	2.67076E-03	5.03363E+00	6.86238E-11
	Std	7.57179E+00	1.55935E+00	6.63172E-03	8.71594E-03	2.28916E+00	6.04315E-12
Rosenbrock	Ave	2.53426E+07	1.51412E+02	1.72588E+02	4.89622E+01	4.59648E+01	2.85371E+01
	Std	1.56600E+07	4.99854E+01	4.19192E+02	5.87337E+01	4.00759E+01	4.18802E-02
Quartic	Ave	1.15934E+01	5.83538E-02	2.64487E-02	1.30656E-01	3.74221E-02	7.24106E-05
	Std	7.71976E+00	1.34839E-02	5.59196E-03	5.25013E-02	1.92040E-02	5.64814E-05
Rastrigin	Ave	1.97323E+01	5.68906E-03	1.09387E-03	5.85295E+00	2.27662E+00	1.27670E-10
	Std	4.50004E+01	7.74115E+00	7.24480E+01	3.21742E+01	3.99808E+00	0.00000E+00
Ackley	Ave	2.05983E+02	7.84538E-03	1.71578E-04	1.06752E-03	1.00090E-02	0.00000E+00
	Std	5.54952E-01	1.17212E-03	2.51166E-04	9.09363E+00	6.02697E-01	1.00524E-11
Levy	Ave	1.77800E+07	5.83263E-05	1.29438E-06	3.11297E-02	2.97280E-01	2.22932E-03
	Std	6.49194E+01	1.08437E-02	7.96341E-05	3.40336E-03	1.02531E-02	0.00000E+00



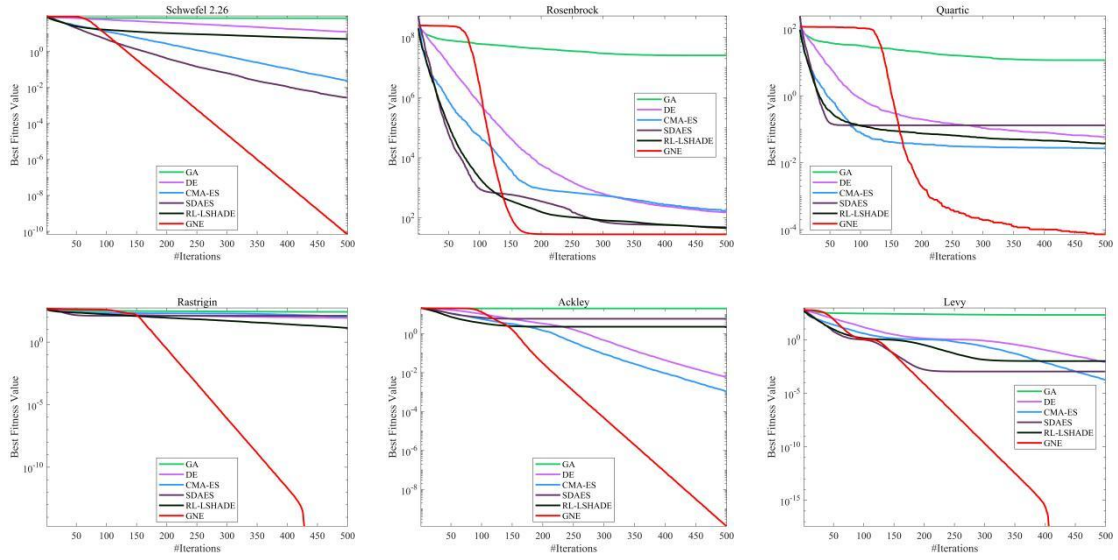


Fig.1 Iterative Convergence Curves of Different Algorithms on Benchmark Functions

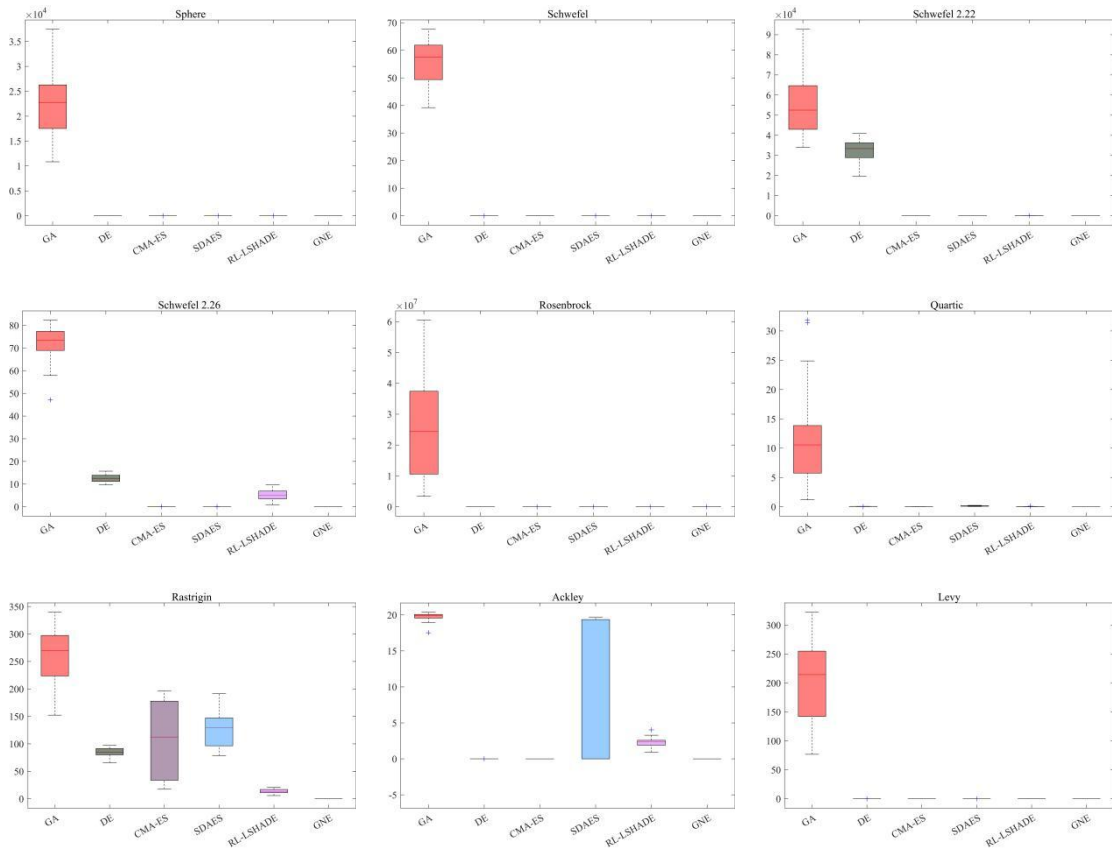
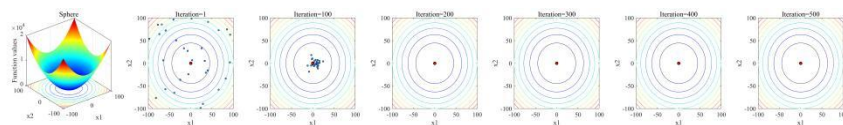


Fig.2 Boxplots of Different Algorithms on Benchmark Functions



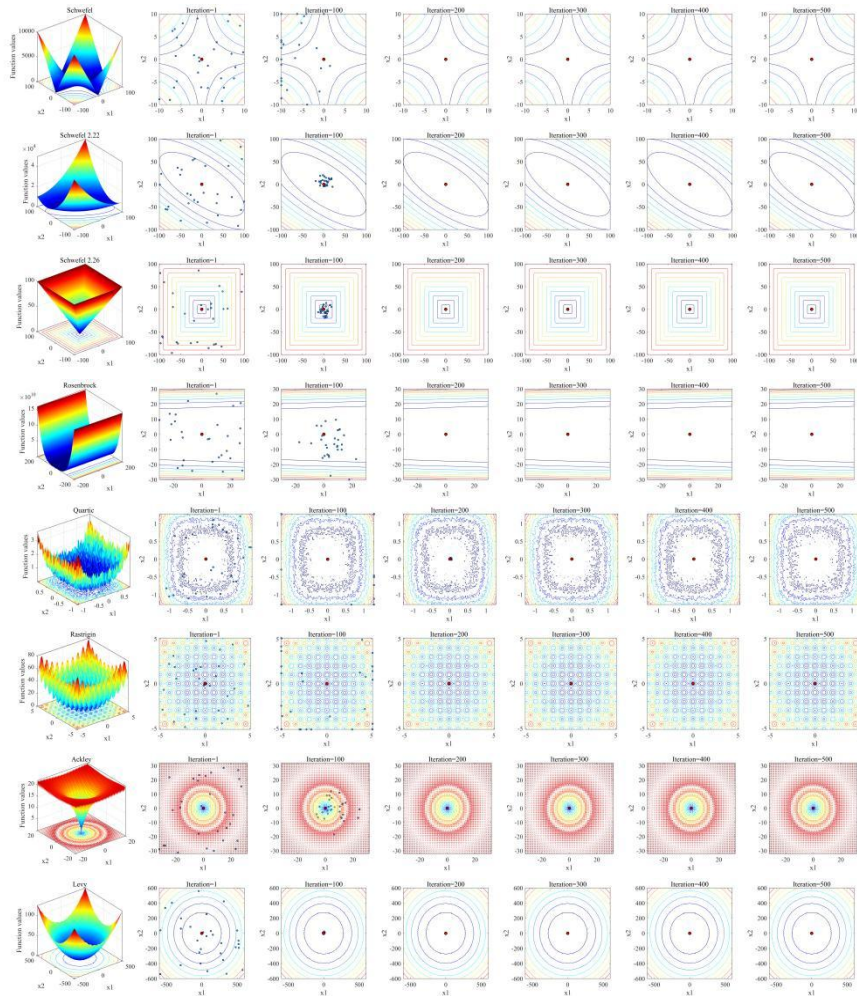


Fig.3 Illustration of GNE's Population Convergence Behavior on Benchmark Functions

Table 1 presents the performance comparison of GNE with other evolutionary algorithms (GA, DE, CMA-ES, SDAES, and RL-SHADE) on various benchmark functions. Across all tested functions, GNE consistently achieves the best results in terms of both average performance and standard deviation, highlighting its precision, stability, and robustness. For example, in Sphere, Schwefel, and Schwefel 2.22, GNE significantly outperforms other algorithms, achieving near-zero average values with the smallest standard deviation, demonstrating its ability to converge rapidly and stably to the global optimum. In multi-modal functions such as Rastrigin and Ackley, where the landscape is highly complex with numerous local optima, GNE excels in maintaining a balance between exploration and exploitation, delivering superior accuracy compared to other methods. On Rosenbrock and Levy, GNE outperforms all other algorithms with its ability to adapt to complex optimization spaces, achieving the lowest error and exhibiting exceptional stability. In contrast, other algorithms show varying levels of performance. While DE and CMA-ES generally perform better than GA on most functions, they often struggle to match GNE's precision and stability. RL-SHADE and SDAES exhibit competitive performance on certain functions, such as Rosenbrock and Ackley, but their results still lack the consistency observed with GNE, particularly in terms of standard deviation, which is crucial for robustness. GA, being the simplest method, demonstrates the weakest performance overall, with higher average errors and larger standard deviations across all functions, indicating its limited capacity

for handling complex or multi-modal optimization problems. **Fig.1**, **Fig.2** and **Fig.3** provide a comprehensive analysis of GNE's performance across benchmark functions, showcasing its superior convergence speed, stability, and population optimization behavior. In **Fig.1**, the iterative convergence curves demonstrate that GNE achieves remarkable efficiency, with its population already concentrated near the global optimum by the 200th iteration, followed by rapid convergence to the final solution. This convergence speed is significantly faster than that of other algorithms, underscoring GNE's ability to effectively balance exploration and exploitation. **Fig.2**, which presents the boxplots of different algorithms, highlights the stability of GNE compared to other methods. GA exhibits poor stability across all functions, while CMA-ES and SDAES show inconsistent stability on certain functions. DE and RL-SHADE maintain relatively high stability, but GNE consistently outperforms them with tight and narrow boxplots, reflecting its reliable and robust performance across all runs and functions. **Fig.3** illustrates GNE's population convergence behavior, where the population is widely distributed across the solution space during the early iterations, demonstrating strong exploration. By the 100th iteration, most individuals have significantly improved, and by the 200th iteration, the entire population has converged near the global optimum, effectively completing the transition from exploration to exploitation. These results highlight GNE's exceptional ability to achieve precision, stability, and efficiency in diverse and challenging optimization scenarios.

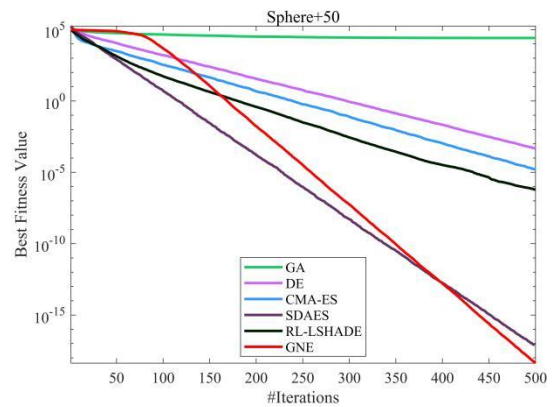
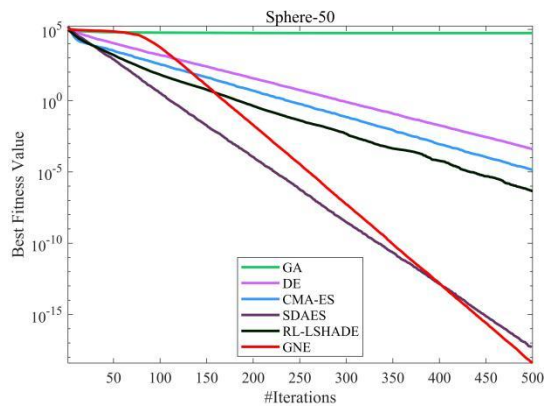
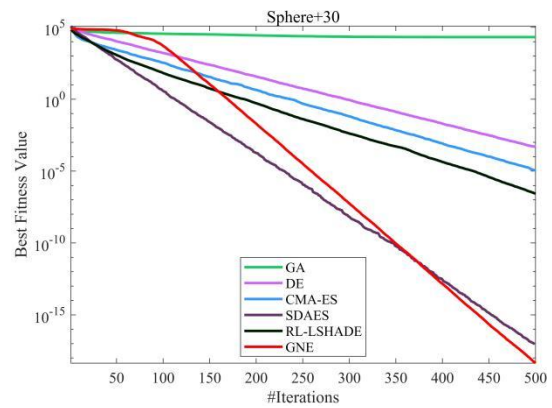
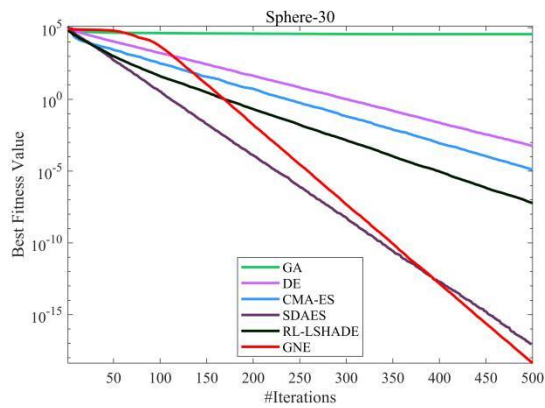
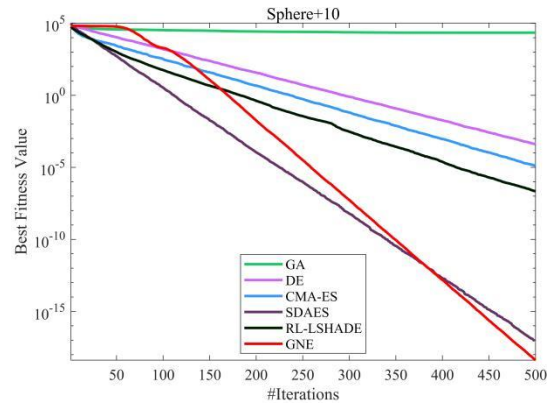
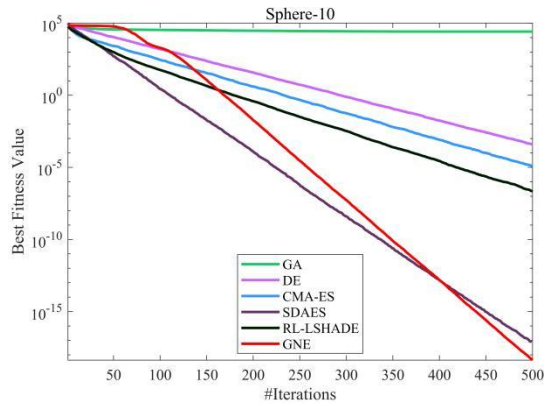
4.2 Robustness of GNE for Optimal Solution Deviation

To verify whether the proposed GNE algorithm exhibits overfitting to the optimal solution, we use the Sphere function as an example. The original optimal solution of the Sphere function is located at the origin (0 point). Subsequently, the optimal solution is intentionally shifted by offsets of -10, -30, -50, -70, -90, +10, +30, +50, +70, and +90. This setup is designed to test the robustness of GNE when the optimal solution of the function deviates from its original position.

Table 2 Performance Comparison of GNE with Other Evolutionary Algorithms on Optimal Solution Deviation Experiment

Benchmark	index	GA	DE	CMA-ES	SDAES	RL-SHADE	GNE
Functions							
Sphere-10	Ave	2.60427E+04	3.93919E-04	1.19525E-05	7.76861E-18	2.16510E-07	4.22342E-19
	Std	7.94117E+03	1.63010E-04	5.66931E-06	9.82239E-18	5.59711E-07	1.33055E-19
Sphere-30	Ave	3.51484E+04	5.49088E-04	1.21482E-05	9.00493E-18	5.83812E-08	4.12159E-19
	Std	1.12106E+04	2.48603E-04	5.81460E-06	1.36931E-17	6.78741E-08	1.11601E-19
Sphere-50	Ave	5.47240E+04	4.01015E-04	1.41491E-05	5.04939E-18	4.55236E-07	3.85523E-19
	Std	1.18952E+04	1.52921E-04	8.43458E-06	6.04090E-18	1.78974E-06	1.17023E-19
Sphere-70	Ave	1.04463E+05	3.49148E-04	1.62857E-05	3.78877E-17	2.03101E-07	4.39068E-19
	Std	2.15951E+04	1.49335E-04	8.96523E-06	9.30949E-17	3.91481E-07	1.26298E-19
Sphere-90	Ave	1.70590E+05	1.31005E-04	1.91661E-05	5.64712E-17	1.14993E-07	4.06468E-19
	Std	2.51158E+04	7.58257E-05	8.09548E-06	1.37591E-16	2.22478E-07	1.00488E-19
Sphere+10	Ave	2.22425E+04	3.96591E-04	1.31001E-05	9.38077E-18	2.16243E-07	4.08853E-19
	Std	8.64563E+03	2.13341E-04	6.11437E-06	1.45305E-17	5.23126E-07	1.01412E-19
Sphere+30	Ave	2.09946E+04	4.87613E-04	1.12573E-05	9.80666E-18	2.70583E-07	4.30217E-19
	Std	8.80330E+03	1.59935E-04	4.81832E-06	1.94273E-17	4.48994E-07	9.90505E-20

Sphere+50	Ave	2.59876E+04	4.59588E-04	1.58881E-05	7.66480E-18	6.20821E-07	4.19507E-19
	Std	1.22350E+04	1.49480E-04	6.11254E-06	9.10011E-18	2.51176E-06	1.19722E-19
Sphere+70	Ave	4.75803E+04	3.36287E-04	1.60471E-05	1.41908E-17	1.08560E-07	3.79376E-19
	Std	1.59513E+04	1.25916E-04	7.52633E-06	2.62725E-17	1.18807E-07	6.79395E-20
Sphere+90	Ave	1.10389E+05	1.41581E-04	1.99578E-05	3.19157E-17	8.24384E-08	3.79301E-19
	Std	2.66768E+04	5.28485E-05	7.86449E-06	7.21745E-17	2.54929E-07	1.55089E-19



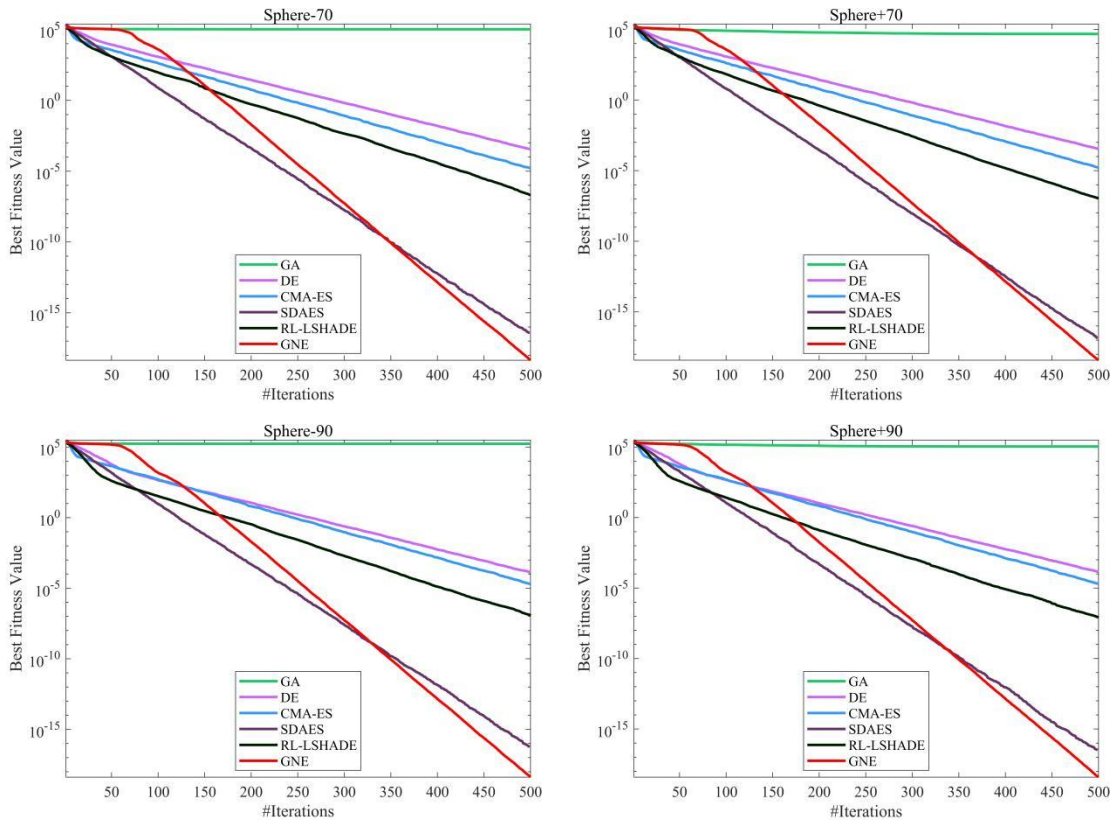
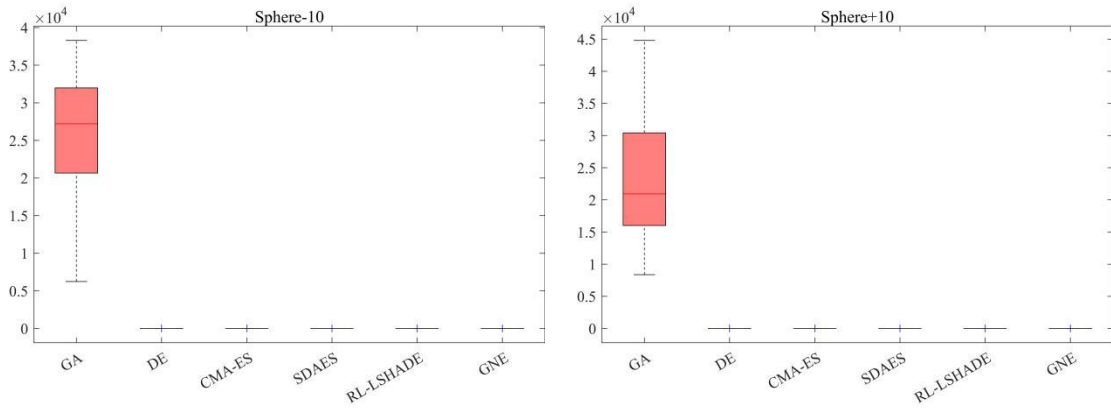


Fig.4 Iterative Convergence Curves of Different Algorithms on Optimal Solution Deviation Experiment



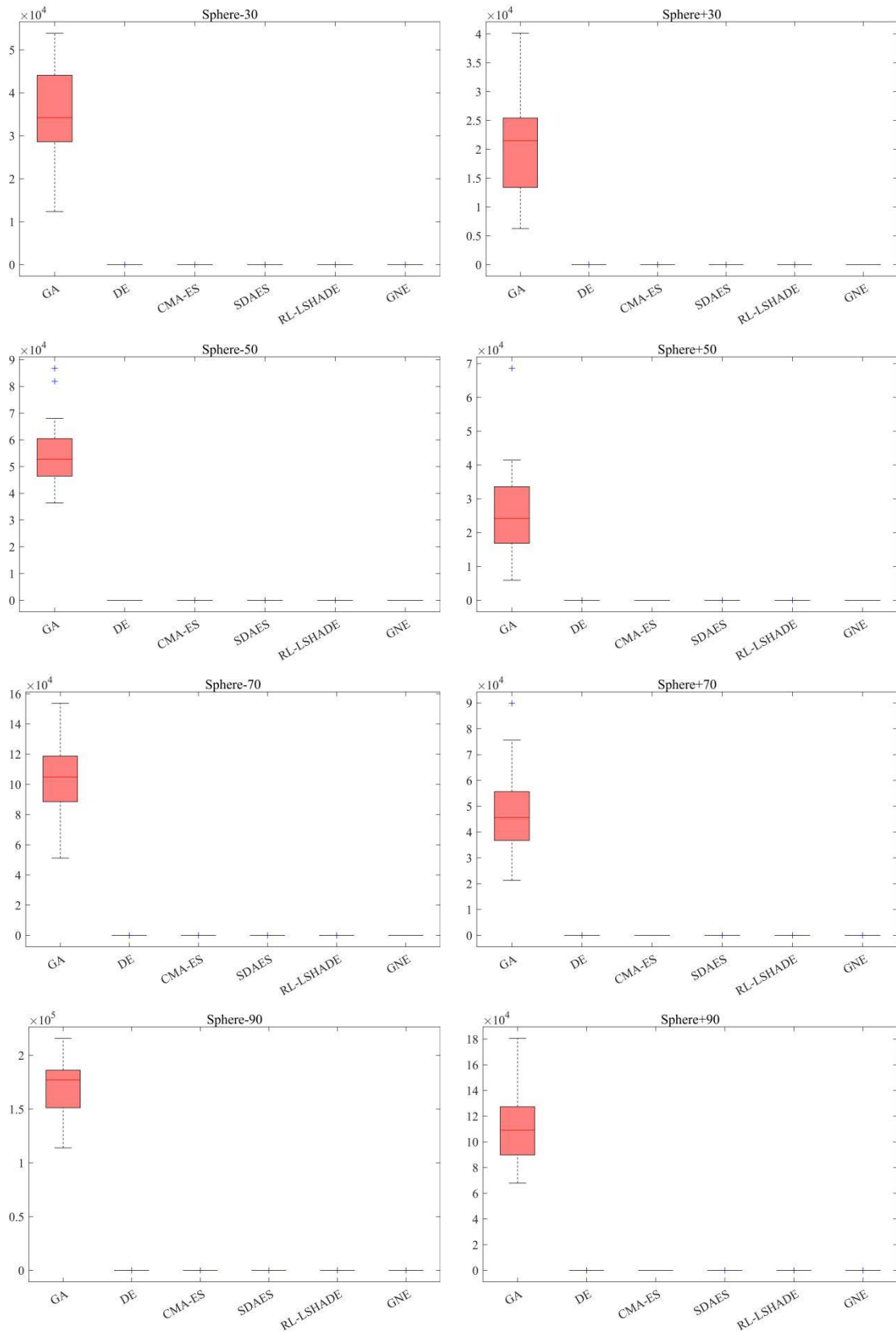


Fig.5 Boxplots of Different Algorithms on Optimal Solution Deviation Experiment

Table 2 presents the performance comparison of GNE with other evolutionary algorithms (GA, DE, CMA-ES, SDAES, and RL-SHADE) under different optimal solution shifts in the Sphere

function. The table shows that GNE consistently achieves the best solution quality, with the smallest averages and the highest stability across all tested shifts, regardless of the magnitude or direction. This highlights GNE’s robustness and adaptability in handling dynamic changes in the solution landscape. **Fig. 4** and **Fig. 5** provide additional evidence for GNE’s superiority. **Fig. 4** illustrates the iterative convergence curves, where GNE demonstrates rapid and stable convergence to the optimal solution under all shift scenarios, significantly outperforming other algorithms. **Fig.5** shows the boxplots for each algorithm, revealing that GNE maintains the tightest distributions, reflecting exceptional stability compared to the wider variability observed in other methods. These results confirm that GNE is not only efficient in finding high-quality solutions but also remarkably robust and generalizable, avoiding overfitting to specific function characteristics.

4.3 Robustness of GNE in Noisy Function Environments

In real-world scenarios, function evaluations are often affected by measurement errors and uncertainties. In this section, we introduce random noise uniformly distributed in the range $[0, 1]$ to the 9 benchmark functions to evaluate the performance of GNE under noisy function conditions. This setup tests the algorithm's robustness when noise is present in the computation of function values.

Table 3 Performance Comparison of GNE with Other Evolutionary Algorithms on Noisy Benchmark Functions

Benchmark Functions	index	GA	DE	CMA-ES	SDAES	RL-SHADE	GNE
Sphere-Noise	Ave	2.30987E+04	2.87248E-01	1.11702E-01	3.64499E-01	2.12554E-01	1.10800E-04
	Std	7.44037E+03	4.20864E-02	2.66908E-02	9.53580E-02	7.92045E-02	8.18719E-05
Schwefel-Noise	Ave	5.48990E+01	6.43432E-01	3.77694E-01	2.51290E+00	6.04009E-01	1.95647E-04
	Std	8.93589E+00	7.48300E-02	4.18089E-02	2.29110E+00	2.94870E-01	1.83940E-04
Schwefel	Ave	5.52486E+04	3.35042E+04	6.29832E-01	8.71936E+00	1.75510E+01	9.11599E-05
2.22-Noise	Std	1.65596E+04	5.03094E+03	2.21713E-01	3.38350E+00	1.15604E+01	7.36643E-05
Schwefel	Ave	7.26737E+01	1.58251E+01	4.10006E-01	4.53696E+00	1.03996E+01	1.55604E-04
2.26-Noise	Std	9.53353E+00	2.93960E+00	5.56076E-02	2.39028E+00	3.62123E+00	1.15110E-04
Rosenbrock-Noise	Ave	2.58700E+07	1.36609E+02	4.90932E+01	9.24291E+01	5.19481E+01	2.88746E+01
	Std	1.44800E+07	6.24535E+01	4.60872E+01	1.24713E+02	4.04622E+01	3.56230E-02
Quartic-Noise	Ave	1.29937E+01	6.07964E-02	2.62375E-02	1.35781E-01	4.01837E-02	5.20526E-05
	Std	1.10570E+01	1.58433E-02	5.59216E-03	4.77874E-02	1.78915E-02	4.97230E-05
Rastrigin-Noise	Ave	2.63218E+02	8.77154E+01	1.23283E+02	1.13305E+02	1.29407E+01	1.00610E-04
	Std	4.26777E+01	7.24183E+00	7.53972E+01	3.74470E+01	3.72993E+00	8.86421E-05
Ackley-Noise	Ave	1.99350E+01	2.81317E+00	7.20179E+00	1.79008E+01	2.69249E+00	1.22486E-04
	Std	5.99326E-01	3.50509E-01	1.00100E+01	6.88517E+00	6.95562E-01	9.02197E-05
Levy-Noise	Ave	1.91159E+02	1.21125E+00	1.10303E+00	1.34588E+00	1.17843E+00	8.36494E-05
	Std	6.32852E+01	2.23799E-02	2.01674E-02	1.05356E-01	7.41337E-02	8.63561E-05

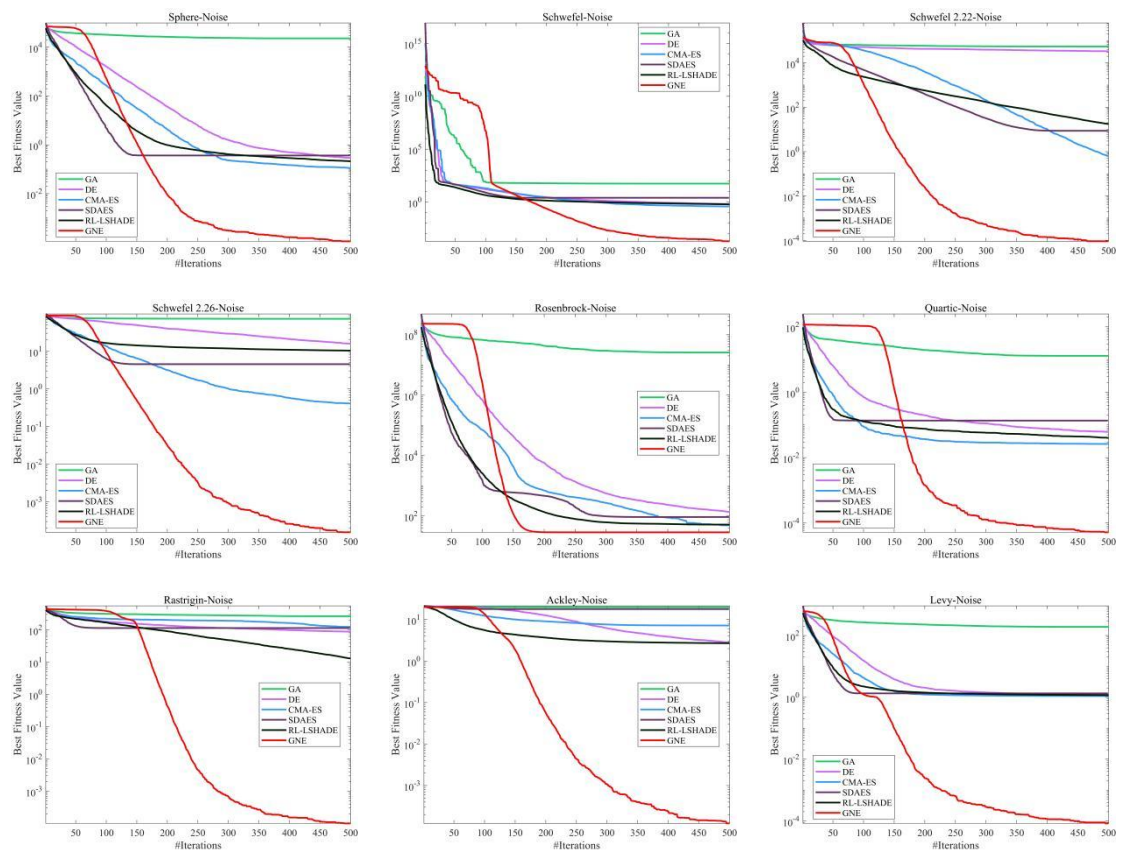


Fig.6 Iterative Convergence Curves of Different Algorithms on Noisy Benchmark Functions

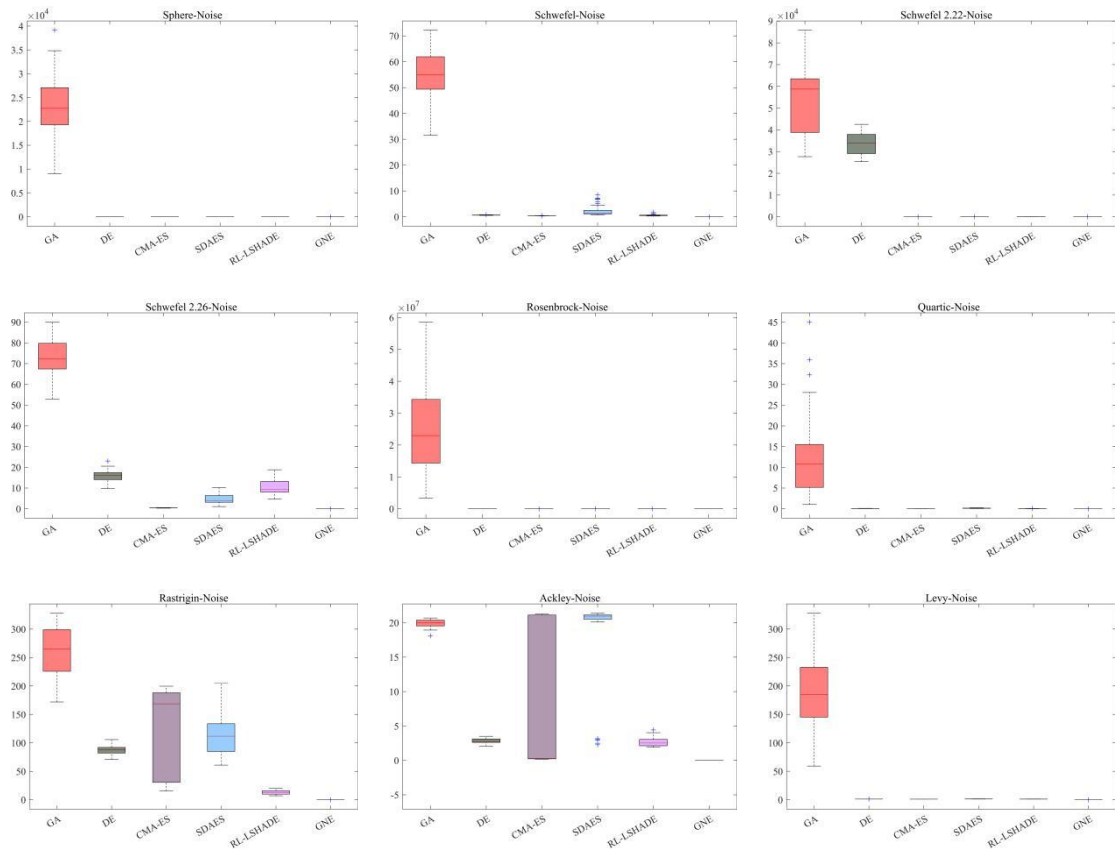


Fig.7 Boxplots of Different Algorithms on Noisy Benchmark Functions

Table 3 highlights the performance of GNE and other evolutionary algorithms (GA, DE, CMA-ES, SDAES, and RL-SHADE) under noisy benchmark functions, showcasing their robustness in handling noisy environments. Compared to the results in Table 1 (noise-free functions), the introduction of random noise significantly impacts the performance of most algorithms. GA and SDAES experience severe performance degradation, with large average errors and high standard deviations across almost all functions, indicating their inability to effectively handle noise. DE and CMA-ES also show reduced performance, particularly in complex multi-modal functions like Rastrigin-Noise and Ackley-Noise, where noise amplifies the difficulty of optimization. RL-SHADE performs relatively better than most algorithms, but its increased variability under noisy conditions makes its results less reliable. In stark contrast, GNE consistently achieves the smallest averages and standard deviations across all noisy benchmark functions, maintaining its superior performance even in the presence of noise. For example, in functions such as Sphere-Noise, Schwefel-Noise, and Quartic-Noise, GNE significantly outperforms other algorithms, demonstrating its robustness and ability to effectively mitigate the influence of noise. Even in challenging scenarios like Rastrigin-Noise and Ackley-Noise, where noise typically causes significant performance degradation, GNE remains highly accurate and stable. This exceptional robustness can be attributed to GNE's advanced filtering mechanism, which efficiently filters out noise from the population information during optimization. By focusing on meaningful genetic information and disregarding noisy or irrelevant components, GNE ensures precise and stable optimization results, even in noisy environments. **Fig. 6** further supports these findings by illustrating the iterative convergence curves for different algorithms under noisy conditions. The convergence speed and precision of many algorithms, such as GA, DE, and CMA-ES, are significantly hindered by noise, with slower convergence and less reliable results. RL-SHADE, while performing better than GA and SDAES, still exhibits fluctuations in convergence behavior under noisy conditions. In contrast, GNE maintains rapid and stable convergence across all noisy functions, consistently achieving near-optimal solutions by the 200th iteration, regardless of the presence of noise. **Fig. 7** provides additional evidence through boxplots, comparing the stability of algorithms across multiple runs. While many algorithms, including CMA-ES and SDAES, exhibit wider variability and reduced stability under noisy conditions, GA shows the largest performance fluctuations, confirming its poor robustness to noise. GNE, however, stands out with the tightest and most consistent boxplots across all noisy functions, demonstrating minimal deviation and exceptional stability. This reinforces GNE's ability to maintain high performance with reduced variability, even when faced with noise.

4.4 Performance of GNE with Different Polynomial Bases

As an extension, we conducted a preliminary evaluation of the performance of the GNE algorithm under 12 different polynomial bases and tested them on the benchmark functions. These polynomial bases, listed in the following order, include: Chebyshev, Bessel, Fibonacci, Fourier, Gegenbauer, Hermite, Jacobi, Laguerre, Legendre, Lucas, Monomial, and Bernstein. This exploration aims to investigate how different polynomial bases influence the performance of the GNE algorithm.

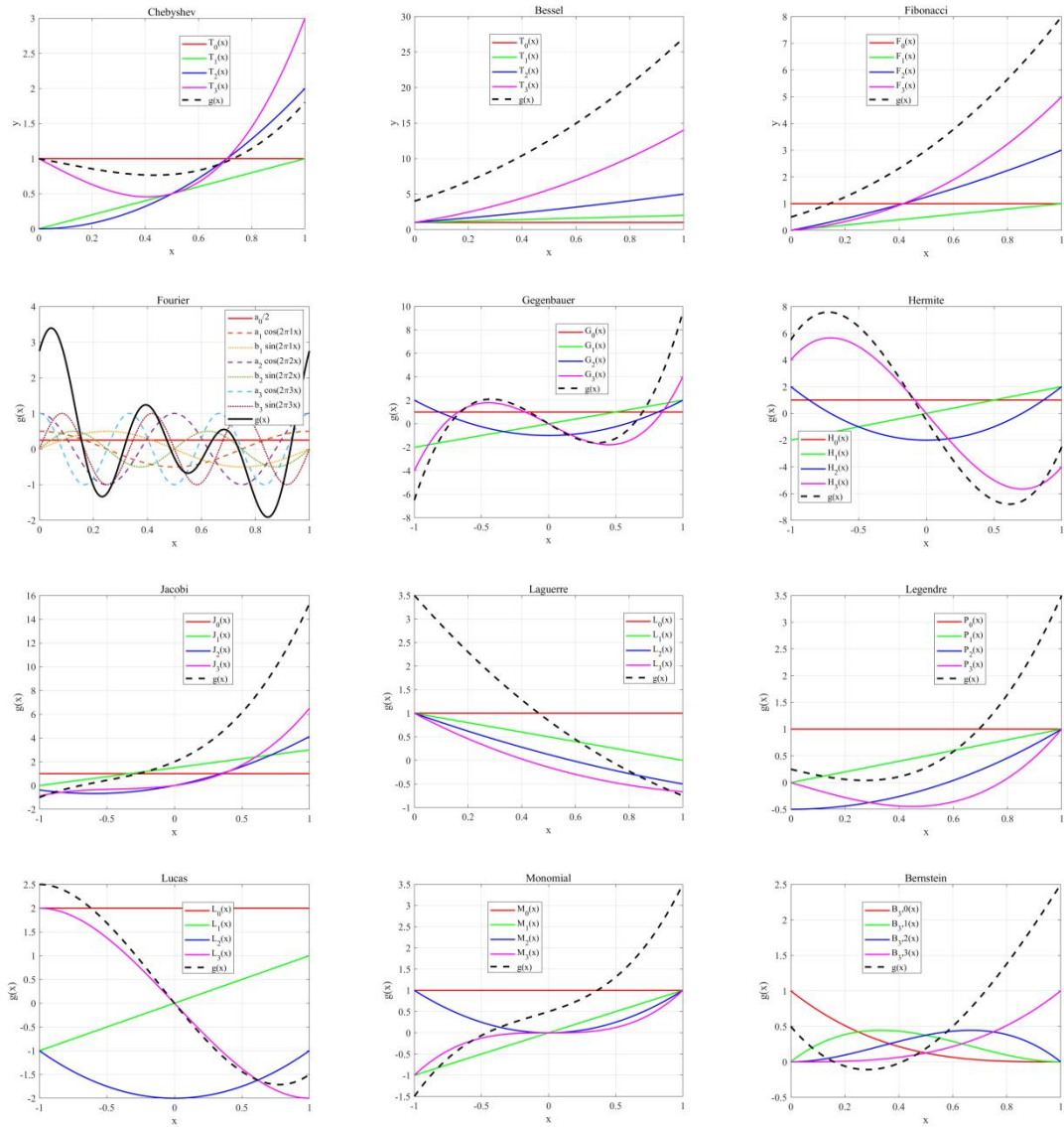


Fig.8 Illustrations of Different Polynomial Bases

Table 4 Performance Comparison of GNE Algorithm Under 12 Different Polynomial Bases

Benchmark	index	GNE-Chebyshev	GNE-Bessel	GNE-Fibonacci	GNE-Fourier	GNE-Gegenbauer	GNE-Hermite	GNE-Jacobi	GNE-Laguerre	GNE-Legendre	GNE-Lucas	GNE-Monomial	GNE-Bernstein
Functions													
Sphere	Ave	3.07763E-20	8.93555E-20	8.40255E-20	3.75872E-19	3.38896E-20	4.18035E-19	7.89867E-20	1.77130E-19	3.95475E-20	3.81814E-19	7.04543E-20	3.70648E-20
	Std	4.22605E-21	1.36594E-20	1.42032E-20	9.91888E-20	6.40722E-21	9.92219E-20	1.22489E-20	2.99154E-20	7.06014E-21	1.01150E-19	1.48369E-20	6.37676E-21
Schwefel	Ave	7.46480E-10	1.31009E-09	1.24663E-09	8.89785E+01	8.00647E-10	7.52850E+01	1.23244E-09	1.87941E-09	8.81956E-10	4.69221E+00	1.13917E-09	8.29579E-10
	Std	6.21576E-11	1.21555E-10	1.13705E-10	2.69543E+01	7.66476E-11	3.42580E+01	1.10387E-10	1.12119E-10	6.42374E-11	2.56529E+00	1.22475E-10	7.81536E-11
Schwefel	Ave	6.34709E-20	1.98217E-19	1.80323E-19	9.24243E+03	7.69945E-20	6.74174E+03	1.71233E-19	3.37200E-19	8.65513E-20	3.55625E+03	1.42511E-19	8.69686E-20
	Std	1.60650E-20	6.65101E-20	4.45323E-20	2.48567E+03	2.07679E-20	2.35815E+03	4.98511E-20	7.09605E-20	2.56478E-20	1.65699E+03	3.95312E-20	2.05185E-20
Schwefel	Ave	6.76219E-11	1.17540E-10	1.10812E-10	2.99317E+01	6.98481E-11	2.23632E+01	1.08642E-10	1.65962E-10	7.64388E-11	1.41664E+01	9.99840E-11	7.46457E-11
	Std	5.69527E-12	8.57202E-12	1.30179E-11	9.34262E+00	6.99991E-12	7.57489E+00	9.85074E-12	1.24187E-11	4.95728E-12	4.89421E+00	9.09269E-12	5.91948E-12
Rosenbrock	Ave	2.85276E+01	2.85139E+01	2.85117E+01	5.25428E+03	2.85122E+01	3.39625E+03	2.85237E+01	2.84633E+01	2.85196E+01	2.56526E+03	2.84977E+01	2.85395E+01
	Std	3.94366E-02	6.11465E-02	5.69611E-02	9.08621E+03	4.94950E-02	5.49728E+03	4.83205E-02	1.36797E-01	6.12486E-02	6.47315E+03	4.87085E-02	5.05735E-02
Quartic	Ave	5.56772E-05	6.93867E-05	6.25252E-05	2.45095E-01	6.05076E-05	2.15226E-01	7.14697E-05	5.67562E-05	5.25906E-05	2.20578E-01	4.52743E-05	6.50835E-05
	Std	5.61449E-05	6.20435E-05	5.48531E-05	8.77195E-02	5.30787E-05	8.94548E-02	6.43987E-05	6.64019E-05	6.25008E-05	6.90282E-02	3.69255E-05	5.57070E-05
Rastrigin	Ave	0.00000E+00	0.00000E+00	0.00000E+00	1.74017E+02	0.00000E+00	1.38431E+02	0.00000E+00	0.00000E+00	0.00000E+00	6.94811E+01	0.00000E+00	0.00000E+00
	Std	0.00000E+00	0.00000E+00	0.00000E+00	4.24181E+01	0.00000E+00	3.12986E+01	0.00000E+00	0.00000E+00	0.00000E+00	1.24245E+01	0.00000E+00	0.00000E+00
Ackley	Ave	1.28867E-10	2.17208E-10	2.04667E-10	1.99610E+01	1.32059E-10	6.56887E+00	1.94184E-10	3.16974E-10	1.42142E-10	2.63083E+00	1.89065E-10	1.42324E-10
	Std	1.31972E-11	2.14377E-11	2.03397E-11	2.16979E-03	1.14377E-11	7.54161E+00	1.98044E-11	2.20514E-11	1.20406E-11	7.27391E-01	2.19166E-11	1.20815E-11
Levy	Ave	7.14756E-03	1.56269E-02	1.74360E-02	8.32912E+00	1.78153E-02	8.27202E+00	3.07535E-02	2.66514E-02	1.61006E-02	6.63603E+00	1.58087E-02	6.03790E-03
	Std	0.00000E+00	0.00000E+00	0.00000E+00	9.25639E-03	0.00000E+00	1.11908E-02	0.00000E+00	0.00000E+00	0.00000E+00	1.77767E-02	0.00000E+00	0.00000E+00

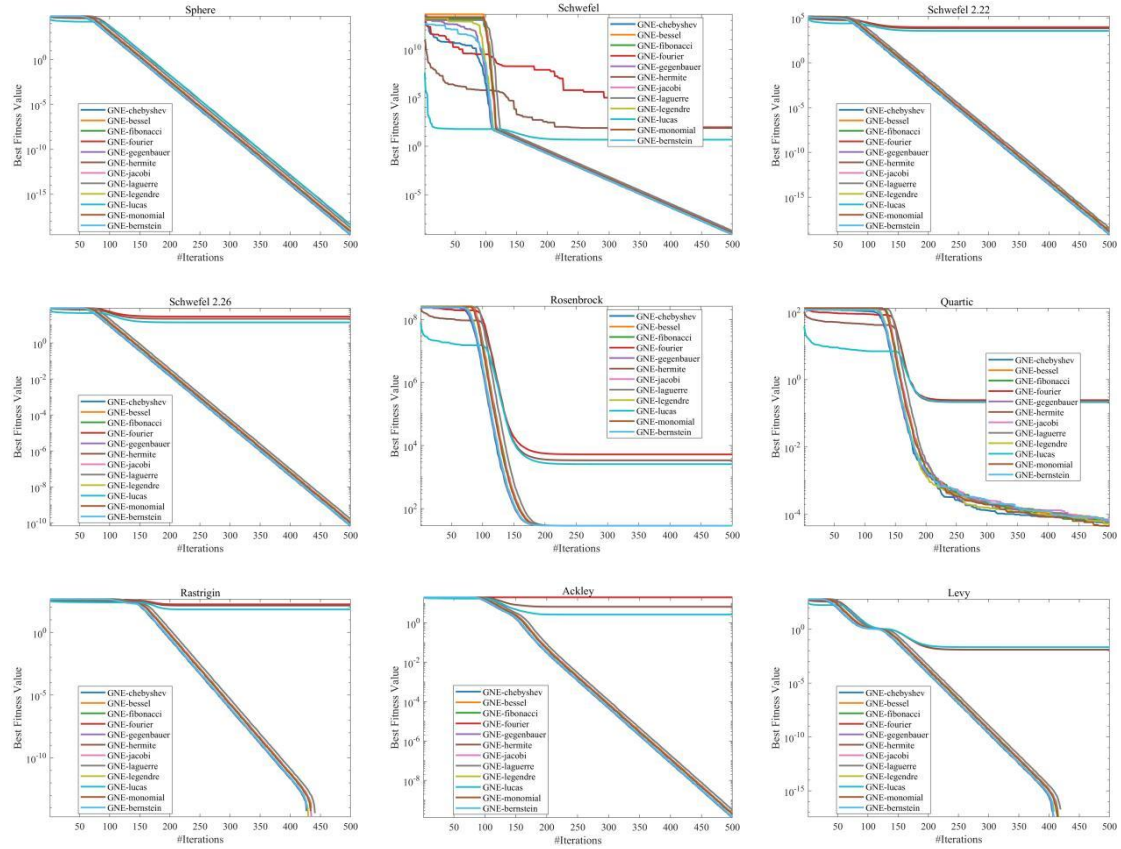


Fig.9 Iterative Convergence Curves of GNE Under Different Polynomial Bases on Benchmark Functions

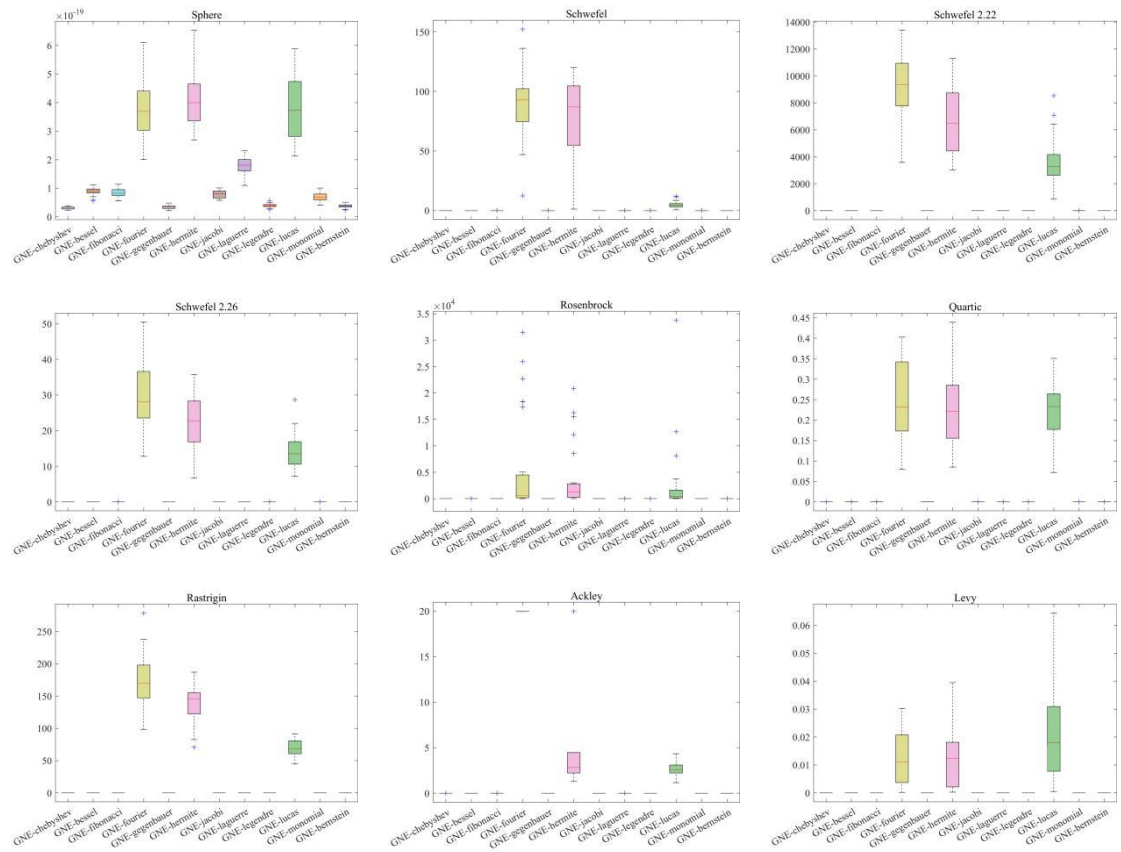


Fig.10 Boxplots of GNE Under Different Polynomial Bases on Benchmark Functions

The performance of GNE under different polynomial bases, as summarized in **Table 4**, highlights significant variations across benchmark functions, with smaller averages and standard deviations indicating better optimization accuracy and stability. Among the polynomial bases tested, Chebyshev, Bernstein, and Legendre consistently deliver the best results, with Chebyshev emerging as the overall top performer. These three bases share a U-shaped frequency-weight distribution, where the weights first decrease and then increase from low to high frequencies. This structure allows them to effectively balance low-frequency stability and high-frequency diversity, enabling precise and robust optimization. For example, in functions like Sphere, Schwefel, and Quartic, these bases achieve the smallest averages and standard deviations, showcasing their superior ability to adapt to diverse optimization landscapes. In contrast, polynomial bases like Bessel, Fibonacci, Jacobi, and Monomial, which emphasize high-frequency components through a monotonic increase in weights, show moderate performance. These bases are well-suited for functions requiring high exploration, such as Schwefel and Ackley, where their focus on high-frequency information helps avoid local optima. However, their performance on stability-dependent functions like Rosenbrock or Quartic is less consistent, often resulting in higher averages and standard deviations compared to the U-shaped bases like Chebyshev or Legendre. Low-frequency dominant bases like Laguerre and Lucas, with weights that decrease monotonically from low to high frequencies, demonstrate strong stability but limited exploration capabilities. While they excel in functions such as Sphere and Rosenbrock, where stability is key, they struggle in multi-modal or high-complexity functions like Rastrigin and Ackley, where exploration plays a more significant role. This trade-off is evident in their higher averages and variability in these scenarios. Bases such as Fourier, Gegenbauer, and Hermite, characterized by oscillatory weight distributions, generally perform poorly. Their fluctuating emphasis across frequencies leads to inconsistent results, particularly in challenging functions like Schwefel 2.22 and Rastrigin, where balanced filtering is crucial. Fourier, for instance, demonstrates instability and slow convergence in functions like Schwefel and Ackley, reflecting its inability to balance exploration and exploitation effectively. **Fig.9**, showcasing the iterative convergence curves, illustrates that bases like Chebyshev, Bernstein, and Legendre converge rapidly and stably across most benchmark functions, consistently achieving near-optimal solutions with minimal fluctuations. In contrast, oscillatory or extreme frequency-weight bases such as Fourier and Laguerre exhibit slower convergence and greater variability, particularly in more complex functions. **Fig.10**, through boxplots, further validates these findings, showing tight and narrow boxplots for Chebyshev, Bernstein, and Legendre, which reflect their reliable and consistent performance. In contrast, bases like Fourier, Gegenbauer, and Hermite exhibit wider boxplots, indicative of higher variability and reduced robustness. Overall, the U-shaped frequency-weight distribution of Chebyshev, Bernstein, and Legendre allows them to achieve a superior balance between low-frequency stability and high-frequency diversity, making them the most effective polynomial bases for GNE. Among these, Chebyshev consistently emerges as the best performer, delivering the most stable and accurate results across all benchmark functions. These findings underscore the importance of selecting a polynomial base with balanced frequency-weight characteristics, with Chebyshev standing out as the optimal choice for most optimization problems.

5. Conclusion

In this work, we introduced Graph Neural Evolution (GNE), a novel algorithm that bridges evolutionary computation and graph neural networks (GNNs) through a unified frequency-domain perspective. By modeling the population updates of evolutionary algorithms as a filtering process on a graph, GNE effectively aggregates high-frequency and low-frequency information, achieving a dynamic balance between exploration and exploitation. This innovative approach not only enhances the interpretability of evolutionary algorithms but also establishes a profound theoretical connection between these two seemingly distinct fields. The experimental results demonstrate the remarkable performance of GNE across various optimization challenges. GNE excels in scenarios involving optimal solution shifts and noisy environments, consistently outperforming state-of-the-art evolutionary algorithms such as GA, DE, CMA-ES, RL-SHADE, and SDAES. Its robustness and adaptability are evident in its ability to maintain high accuracy, stability, and convergence speed, even under challenging conditions. By effectively balancing exploration and exploitation, GNE delivers superior optimization results for both unimodal and multimodal functions, showcasing its potential as a versatile and powerful optimization framework. Despite these achievements, there is significant room for improvement and further exploration. The polynomial filters employed in this study were selected based on initial experimentation and are not necessarily optimal for all problem types. Future work could focus on developing adaptive filtering mechanisms, where the polynomial basis evolves dynamically during the optimization process. For instance, filters could emphasize high-frequency components in the early stages to enhance exploration and gradually shift toward low-frequency components in later stages to strengthen exploitation. Additionally, the potential of hybrid filters — combining multiple polynomial bases — or non-polynomial filters could be explored to further enhance GNE's performance. Another promising avenue lies in extending GNE to multi-objective optimization problems, enabling it to handle more complex real-world tasks with competing objectives. Hierarchical frameworks or problem-specific adaptations could further broaden GNE's applicability to challenging optimization scenarios. Furthermore, GNE's ability to act as a general-purpose optimizer opens up exciting opportunities in machine learning, such as hyperparameter tuning, neural architecture search, and combinatorial optimization, as well as applications in engineering design and operational research. These extensions could significantly enhance GNE's impact across diverse fields. This work also contributes to a deeper understanding of the relationship between evolutionary algorithms and GNNs. By drawing parallels between the filtering of genetic information in evolutionary algorithms and the frequency-based information aggregation in spectral GNNs, we establish a theoretical foundation for cross-disciplinary innovation. Future research could explore how evolutionary concepts, such as genetic recombination or adaptive mutation strategies, can inspire improvements in GNN architectures, mitigating issues such as oversmoothing and improving their generalization capabilities. In summary, we present Graph Neural Evolution (GNE) as a significant step forward in evolutionary computation and graph-based learning. By combining frequency-domain insights with practical algorithm design, GNE redefines the core principles of exploration and exploitation in optimization. Its robustness, adaptability, and performance across diverse scenarios highlight its potential for broad applicability. Looking forward, the outlined directions for improvement and exploration offer exciting possibilities for advancing GNE's capabilities, inspiring future research,

and broadening its applications in optimization, machine learning, and real-world problem-solving. We hope that this work will ignite further innovation in the interplay between evolutionary computation and graph neural networks, paving the way for transformative progress in both fields.

References

1. Rosenblatt, F., *The perceptron: a probabilistic model for information storage and organization in the brain*. Psychological review, 1958. **65**(6): p. 386.
2. Rumelhart, D.E., G.E. Hinton, and R.J. Williams, *Learning representations by back-propagating errors*. nature, 1986. **323**(6088): p. 533-536.
3. LeCun, Y., *Generalization and network design strategies*. Connections in Perspective, 1989.
4. McCulloch, W.S. and W. Pitts, *A logical calculus of the ideas immanent in nervous activity*. The bulletin of mathematical biophysics, 1943. **5**: p. 115-133.
5. Hopfield, J.J., *Neural networks and physical systems with emergent collective computational abilities*. Proceedings of the national academy of sciences, 1982. **79**(8): p. 2554-2558.
6. Hebb, D.O., *The organization of behavior: A neuropsychological theory*. 2005: Psychology press.
7. Cybenko, G., *Approximation by superpositions of a sigmoidal function*. Mathematics of control, signals and systems, 1989. **2**(4): p. 303-314.
8. Holland, J.H., *Genetic algorithms*. Scientific american, 1992. **267**(1): p. 66-73.
9. Wright, S., *The roles of mutation, inbreeding, crossbreeding, and selection in evolution*. 1932.
10. Darwin, C., *Origin of the Species*, in *British Politics and the environment in the long nineteenth century*. 2023, Routledge. p. 47-55.
11. Kipf, T.N. and M. Welling, *Semi-supervised classification with graph convolutional networks*. arXiv preprint arXiv:1609.02907, 2016.
12. Veličković, P., et al., *Graph attention networks*. arXiv preprint arXiv:1710.10903, 2017.
13. Lewontin, R.C., *The genetic basis of evolutionary change*. 1974.
14. Kauffman, S. and S. Levin, *Towards a general theory of adaptive walks on rugged landscapes*. Journal of theoretical Biology, 1987. **128**(1): p. 11-45.
15. Smith, J.M., *Evolution and the Theory of Games*, in *Did Darwin get it right? Essays on games, sex and evolution*. 1982, Springer. p. 202-215.
16. Lewontin, R.C., *The units of selection*. Annual review of ecology and systematics, 1970: p. 1-18.
17. Gillespie, J.H., *Natural selection for within-generation variance in offspring number*. Genetics, 1974. **76**(3): p. 601-606.
18. Bäck, T. and H.-P. Schwefel, *An overview of evolutionary algorithms for parameter optimization*. Evolutionary computation, 1993. **1**(1): p. 1-23.
19. Eiben, A.E. and C.A. Schippers, *On evolutionary exploration and exploitation*. Fundamenta Informaticae, 1998. **35**(1-4): p. 35-50.
20. March, J.G., *Exploration and exploitation in organizational learning*. Organization science, 1991. **2**(1): p. 71-87.
21. Yao, X., Y. Liu, and G. Lin, *Evolutionary programming made faster*. IEEE Transactions on Evolutionary computation, 1999. **3**(2): p. 82-102.

22. Sareni, B. and L. Krahenbuhl, *Fitness sharing and niching methods revisited*. IEEE transactions on Evolutionary Computation, 1998. **2**(3): p. 97-106.
23. Scarselli, F., et al., *The graph neural network model*. IEEE transactions on neural networks, 2008. **20**(1): p. 61-80.
24. Hamilton, W., Z. Ying, and J. Leskovec, *Inductive representation learning on large graphs*. Advances in neural information processing systems, 2017. **30**.
25. Li, Q., Z. Han, and X.-M. Wu. *Deeper insights into graph convolutional networks for semi-supervised learning*. in *Proceedings of the AAAI conference on artificial intelligence*. 2018.
26. 鈴木大慈, *Graph neural networks exponentially lose expressive power for node classification*. ICLR2020, 2020. **8**.
27. Chen, M., et al. *Simple and deep graph convolutional networks*. in *International conference on machine learning*. 2020. PMLR.
28. Liu, M., H. Gao, and S. Ji. *Towards deeper graph neural networks*. in *Proceedings of the 26th ACM SIGKDD international conference on knowledge discovery & data mining*. 2020.
29. Rong, Y., et al., *Dropedge: Towards deep graph convolutional networks on node classification*. arXiv preprint arXiv:1907.10903, 2019.
30. Liu, X., et al., *Graph neural networks with adaptive residual*. Advances in Neural Information Processing Systems, 2021. **34**: p. 9720-9733.
31. Eiben, A.E. and J.E. Smith, *Introduction to evolutionary computing*. 2015: Springer.
32. Mahfoud, S.W., *Niching methods for genetic algorithms*. 1995: University of Illinois at Urbana-Champaign.
33. Shi, Y. and R.C. Eberhart. *Parameter selection in particle swarm optimization*. in *Evolutionary Programming VII: 7th International Conference, EP98 San Diego, California, USA, March 25–27, 1998 Proceedings 7*. 1998. Springer.
34. Das, S. and P.N. Suganthan, *Differential evolution: A survey of the state-of-the-art*. IEEE transactions on evolutionary computation, 2010. **15**(1): p. 4-31.
35. Wang, G., et al., *Direct multi-hop attention based graph neural network*. arXiv preprint arXiv:2009.14332, 2020: p. 137.
36. Bo, D., et al. *Beyond low-frequency information in graph convolutional networks*. in *Proceedings of the AAAI conference on artificial intelligence*. 2021.
37. Chen, D., et al. *Measuring and relieving the over-smoothing problem for graph neural networks from the topological view*. in *Proceedings of the AAAI conference on artificial intelligence*. 2020.
38. Zhao, L. and L. Akoglu, *Pairnorm: Tackling oversmoothing in gnns*. arXiv preprint arXiv:1909.12223, 2019.
39. Zhang, P., et al. *TransGNN: Harnessing the collaborative power of transformers and graph neural networks for recommender systems*. in *Proceedings of the 47th International ACM SIGIR Conference on Research and Development in Information Retrieval*. 2024.
40. Yang, J., et al., *Graphformers: Gnn-nested transformers for representation learning on textual graph*. Advances in Neural Information Processing Systems, 2021. **34**: p. 28798-28810.
41. Shirzad, H., et al. *Expformer: Sparse transformers for graphs*. in *International Conference on Machine Learning*. 2023. PMLR.

42. Wu, Q., et al., *Simplifying and empowering transformers for large-graph representations*. Advances in Neural Information Processing Systems, 2024. **36**.
43. Bruna, J., et al., *Spectral networks and locally connected networks on graphs*. arXiv preprint arXiv:1312.6203, 2013.
44. Defferrard, M., X. Bresson, and P. Vandergheynst, *Convolutional neural networks on graphs with fast localized spectral filtering*. Advances in neural information processing systems, 2016. **29**.
45. Wu, F., et al. *Simplifying graph convolutional networks*. in *International conference on machine learning*. 2019. PMLR.
46. Dong, X., et al., *Learning graphs from data: A signal representation perspective*. IEEE Signal Processing Magazine, 2019. **36**(3): p. 44-63.
47. Chen, Z., et al., *Bridging the gap between spatial and spectral domains: A unified framework for graph neural networks*. ACM Computing Surveys, 2023. **56**(5): p. 1-42.
48. Wang, X. and M. Zhang. *How powerful are spectral graph neural networks*. in *International conference on machine learning*. 2022. PMLR.
49. Bo, D., et al., *A survey on spectral graph neural networks*. arXiv preprint arXiv:2302.05631, 2023.
50. Zheng, S., et al., *Node-oriented spectral filtering for graph neural networks*. IEEE Transactions on Pattern Analysis and Machine Intelligence, 2023.
51. He, M., Z. Wei, and H. Xu, *Bernnet: Learning arbitrary graph spectral filters via bernstein approximation*. Advances in Neural Information Processing Systems, 2021. **34**: p. 14239-14251.
52. Storn, R. and K. Price, *Differential evolution—a simple and efficient heuristic for global optimization over continuous spaces*. Journal of global optimization, 1997. **11**: p. 341-359.
53. Hansen, N., S.D. Müller, and P. Koumoutsakos, *Reducing the time complexity of the derandomized evolution strategy with covariance matrix adaptation (CMA-ES)*. Evolutionary computation, 2003. **11**(1): p. 1-18.
54. He, X., et al., *Large-scale evolution strategy based on search direction adaptation*. IEEE Transactions on Cybernetics, 2019. **51**(3): p. 1651-1665.
55. Zhang, H., et al., *Learning adaptive differential evolution by natural evolution strategies*. IEEE Transactions on Emerging Topics in Computational Intelligence, 2022. **7**(3): p. 872-886.
56. Wu, Z., et al., *A comprehensive survey on graph neural networks*. IEEE transactions on neural networks and learning systems, 2020. **32**(1): p. 4-24.

A Appendix

A.1 Description of Benchmark Functions

This section provides an overview of the benchmark functions used to evaluate the performance of optimization algorithms. These functions are fundamental tools in testing the efficiency, robustness, and versatility of optimization methods across a wide range of scenarios. Each function presents unique characteristics, such as unimodal or multimodal landscapes, smooth or discontinuous surfaces, and varying levels of complexity. **Table 5** summarizes the mathematical expressions, variable bounds, dimensionality, and key characteristics of these benchmark functions.

Table 5 Benchmark Functions Used for Optimization Algorithm Evaluation

Function Name	Mathematical Expression	Bounds	Dim	Characteristics
Sphere	$f(x) = \sum_{i=1}^n x_i^2$	[-100,100]	30	It features a smooth, symmetric, and parabolic surface, making it one of the most fundamental benchmarks for optimization algorithms. It is used to test convergence efficiency, as the global minimum is located at the origin, where all variables are zero.
Schwefel	$f(x) = \sum_{i=1}^n x_i + \prod_{i=1}^n x_i $	[-10,10]	30	This function combines linear summation and multiplicative interactions of the absolute values of variables. Its discontinuous nature and complex structure make it ideal for testing an algorithm's ability to handle mixed landscapes and nonlinear interactions between variables.
Schwefel 2.22	$f(x) = \sum_{i=1}^n (\sum_{j=1}^i x_j)^2$	[-100,100]	30	This function combines linear summation and multiplicative interactions of the absolute values of variables. Its discontinuous nature and complex structure make it ideal for testing an algorithm's ability to handle mixed landscapes and nonlinear interactions between variables.
Schwefel 2.26	$f(x) = \max(x_i), i = 1, \dots, n$	[-100,100]	30	This function focuses on the maximum absolute value among all variables, making it a challenging problem for optimization. It tests robustness against extreme values and an algorithm's ability to converge toward the largest feature in the search space.
Rosenbrock	$f(x) = \sum_{i=1}^{n-1} [100(x_{i+1} - x_i^2)^2 + (x_i - 1)^2]$	[-30,30]	30	Known as the "banana function" due to its narrow, curved valley, this function tests precision and local search efficiency. The global minimum lies in the valley, which requires the algorithm to navigate challenging, non-linear paths to converge effectively.
Quartic	$f(x) = \sum_{i=1}^n ix_i^4 + rand$	[-1.28,1.28]	30	This unimodal function incorporates random noise to simulate real-world optimization challenges. It is used to evaluate an algorithm's ability to achieve robust convergence in noisy environments.
Rastrigin	$f(x) = \sum_{i=1}^n [x_i^2 - 10\cos(2\pi x_i) + 10]$	[-5.12,5.12]	30	This multimodal function features numerous local optima, making it a challenging problem for optimization algorithms. It requires a balance between exploration to avoid local minima and exploitation to converge to the global minimum.
Ackley	$f(x) = -20\exp(-0.2\sqrt{\frac{1}{n}\sum_{i=1}^n x_i^2}) - \exp(\frac{1}{n}\sum_{i=1}^n \cos(2\pi x_i)) + 20 + e$	[-32,32]	30	This function is highly multimodal, with a nearly flat outer region and sharp global minima. It tests an algorithm's ability to explore complex landscapes and converge efficiently despite the presence of numerous local optima.
Levy	$f(x) = \frac{\sum_{i=1}^n x_i^2}{4000} - \prod_{i=1}^n \cos(\frac{x_i}{\sqrt{i}}) + 1$	[-600,600]	30	This function is highly multimodal, with a nearly flat outer region and sharp global minima. It tests an algorithm's ability to explore complex landscapes and converge efficiently despite the presence of numerous local optima.

A.2 Description of Polynomial Bases and Coefficients

In this section, we provide a comprehensive overview of the polynomial bases employed in constructing filters for the GNE algorithm, along with the associated coefficients used during experimentation. These polynomial bases offer diverse frequency characteristics, enabling the design of filters that emphasize low frequencies, high frequencies, or a balanced frequency distribution. The coefficients used for each basis were selected based on initial exploratory studies rather than exhaustive optimization, providing a foundation for understanding the influence of different polynomial bases on the performance of the GNE algorithm. The detailed mathematical definitions, coefficients, and key characteristics of these bases are summarized in **Table 6**, providing insights into how each polynomial base contributes to the construction of effective filters and their potential applications in optimization tasks.

Table 6 Polynomial Bases Used in GNE Algorithm and Their Characteristics

Polynomial	Mathematical Definition	Coefficients Used	Key Characteristics
Basis			
Chebyshev	$T_0(x) = 1, T_1(x) = x, T_2(x) = 2x^2 - 1, T_3(x) = 4x^3 - 3x$	g $= 0.5T_0 + 0.3T_1$ $+ 0.25T_2 + 0.5T_3$	U-shaped weight distribution; smooth and balanced filtering for stability.
Bessel	$B_0(x) = 1, B_1(x) = 1 + x, B_2(x) = 1 + 3x + x^2, B_3(x) = 1 + 6x + 6x^2 + x^3$	g $= 0.5B_0 + 1.5B_1$ $+ 0.5B_2 + 1.5B_3$	High-frequency emphasis; suitable for exploratory optimization.
Bernstein	$B_0(x) = (1 - x)^3, B_1(x) = 3x(1 - x)^2, B_2(x) = 3x^2(1 - x), B_3(x) = x^3$	g $= 0.7B_0 - 1.0B_1$ $+ 0.5B_2 + 2.5B_3$	U-shaped weight distribution; extreme value emphasis for robust optimization.
Fibonacci	$F_0(x) = 1, F_1(x) = x, F_2(x) = x^2 + 2x, F_3(x) = x^3 + 3x^2 + x$	g $= 0.5F_0 + F_1 + 0.5F_2$ $+ F_3$	High-frequency emphasis; promotes exploration in the search space.
Fourier	$A_0(x) = \frac{1}{2}, A_k(x) = \cos(2kx), B_k(x) = \sin(2kx), k = 1, 2, 3$	g $= A_0 + 0.5A_1 + A_2$ $+ 0.8A_3 + 0.3B_1$ $+ 0.6B_2 + 0.9B_3$	Oscillatory behavior; captures diverse frequencies effectively.
Gegenbauer	$G_0(x) = 1, G_1(x) = 2\alpha x, G_2(x) = \alpha(2\alpha + 1)x^2 - \alpha, G_3(x) = (2\alpha + 3)(\alpha + 1)x^3 - 3(\alpha + 1)x, \alpha = 1$	g $= 0.5G_0 + G_1 + 0.5G_2$ $+ G_3$	Balanced filtering; adapts well to general-purpose optimization problems.
Hermite	$H_0(x) = 1, H_1(x) = 2x, H_2(x) = 4x^2 - 2, H_3(x) = 8x^3 - 12x$	g $= 0.5H_0 + H_1 + 0.5H_2$ $+ H_3$	High-frequency emphasis; useful for capturing detailed features.
Jacobi	$J_0(x) = 1, J_1(x) = \frac{1}{2}[2(\alpha + 1) + (\alpha + \beta + 2)x], J_2(x) = \frac{1}{2}(\alpha + 1)(\alpha + 2)x^2 + (\alpha + 1)(\beta + 1)x + \frac{1}{2}(\alpha + 1)(\beta - \alpha), J_3(x) = \frac{1}{6}(\alpha + 1)(\alpha + 2)(\alpha + 3)x^3 + \frac{1}{2}(\alpha + 1)(\alpha + 2)(1 + \beta)x^2 + \frac{1}{2}(\alpha + 1)(2 + \beta - \alpha)x + \frac{1}{6}(\alpha + 1)(\beta - \alpha), \alpha = \frac{1}{2}, \beta = \frac{1}{2}$	g $= 0.5J_0 + J_1 + 0.5J_2$ $+ 1.5J_3$	Configurable emphasis; adjusts well to diverse optimization challenges.
Laguerre	$L_0(x) = 1, L_1(x) = 1 - x, L_2(x) = 0.5(x^2 - 4x + 2), L_3(x) = \frac{x^3 - 9x^2 + 18x - 6}{6}$	g $= 0.5L_0 + L_1 + 0.5L_2$ $+ 1.5L_3$	Low-frequency emphasis; focuses on exploitation and precision.

Legendre	$P_0(x) = 1, P_1(x) = x, P_2(x) = 0.5(3x^2 - 1), P_3(x) = 0.5(5x^3 - 3x)$	g $= 0.5P_0 + P_1 + 0.5P_2$ $+ 1.5P_3$	U-shaped weight distribution; balances low and high frequencies effectively.
Lucas	$L_0(x) = 2, L_1(x) = x, L_2(x) = x^2 - 2, L_3(x) = x^3 - 3x$	g $= 0.5L_0 + L_1 + 0.5L_2$ $+ 1.5L_3$	High-frequency emphasis; promotes exploration in optimization tasks.
Monomial	$M_0(x) = 1, M_1(x) = x, M_2(x) = x^2, M_3(x)$	g $= 0.5M_0 + M_1 + 0.5M_2$ $+ 1.5M_3$	High-frequency emphasis; simple and intuitive for exploration-focused applications.